

Two lobe non-recessed roughened hybrid journal bearing – A comparative study

Satish C. Sharma^{a,1}, Prashant B. Kushare^{b,*}

^a Department of Mechanical and Industrial Engineering, Tribology Laboratory, Indian Institute of Technology, Roorkee 247667, India

^b Mechanical Engineering Department, K.K. Wagh Institute of Engineering Education and Research, Nashik 422003, India

ARTICLE INFO

Article history:

Received 28 July 2014

Received in revised form

1 October 2014

Accepted 31 October 2014

Available online 15 November 2014

Keywords:

Surface roughness

Two lobe

Non-recessed bearing

Restrictor

ABSTRACT

The present paper examines the influence of surface roughness on the performance of two lobe hybrid journal bearing. The performance characteristics of two lobe journal bearings compensated with different types of flow control devices such as orifice, capillary, constant flow valve and slot restrictors, have been presented for different forms of roughness patterns such as transverse, longitudinal, isotropic and smooth surface. The results of the study indicate that roughness orientation significantly affects the performance of bearing system. Further, results indicates that, a proper selection of roughness pattern parameter, offset factor and compensating device is essential to enhance the bearing performance.

© 2014 Elsevier Ltd. All rights reserved.

1. Introduction

Over the last couple of decades, non-recessed circular hybrid journal bearings have gained tremendous popularity over recessed bearings due to their improved performance characteristics at low and high speed. As a result of this, hole entry and slot entry hybrid journal bearings are widely employed in many engineering applications [1–4].

The performance of externally pressurized bearing is greatly dependent on the type of flow control device as it supplies the lubricant under pressure. Consequently, different restrictors such as orifice, constant flow valve, capillary, slot entry etc. have been developed and employed in bearing systems. However, under stringent and critical operating condition, the bearings are often subjected to variations in stiffness and load. Under such circumstances, choice of a suitable flow controlling device becomes critical. Further, the accuracy in manufacturing of restrictors for hole entry and slot entry bearing plays vital role because of required precision in tolerance on the restrictor dimensions. Many studies concerning the influence of different flow control devices on bearing performance have been reported in the published literature [1–2,5–6]. The available studies mainly concern about the circular recessed/non-recessed and non-circular multirecess hybrid journal bearing systems and noticeably point out that the selection and type of compensating device play a vital role in enhancing of the bearing performance. The circular journal

bearings are prone to oil whirl instability. However, this problem can be suppressed by the use of multilobes in bearing designs [7,9–16]. Among the different types of multilobe journal bearings, two lobe journal bearing configuration is more popular owing to its better damping and anti-whirl capabilities. As a result of this, several experimental and theoretical studies related to two lobe bearing configurations have been reported in the published literature [9,11–14]. Lund and Thomsen [9] exhaustively studied the elliptical hydrodynamic journal bearing and provided vital information on the values of length to diameter ratios. Malik [12] presented an analytical study of lobed journal bearing and provided the design data, considering various aspects over the broad range of load condition. More recently, Rahmatabadi et al. [15] carried out the study of two lobe, three lobe and four-lobe hydrodynamic bearings operated with micropolar lubricants. It was reported that the use of micropolar lubricant enhances the static performance characteristics. These days, many studies concerning multilobe hybrid journal bearing systems have been reported in the published literature [16–21,22–24]. An experimental study on water lubricated multi-recessed bearing was carried out by San Andres [16]. He investigated the combined effect of geometric asymmetry and recess position on the dynamic coefficients and whirl frequency. Ghosh and Satish [17,18] carried out a study to determine the dynamic performance characteristics of 3-lobe and 4-lobe recessed hybrid journal bearings for different values of offset factors using the small amplitude perturbation method. The result of their study indicates that the non-circular hybrid bearings with a ratio of maximum to minimum clearance ratio greater than one provide improved stability than the circular bearing configuration.

* Corresponding author. Mobile: +91 98 9042 6679.

E-mail addresses: sshmefme@iitr.ernet.in (S.C. Sharma), pbkushare@gmail.com (P.B. Kushare).

¹ Tel.: +91 13 3228 6609; fax: +91 13 3228 5665.

Nomenclature

a_b	bearing land width, mm
c	radial clearance, mm
e	journal eccentricity, mm
E	Young's modulus of elasticity, N mm ⁻²
F	fluid film reaction ($\partial h/\partial t \neq 0$), N
F_x, F_z	components of fluid film reactions in X and Z direction ($\partial h/\partial t \neq 0$), N
F_o	fluid film reaction ($\partial h/\partial t = 0$), N
C_1	clearance due to circumscribed circle on the bearing, mm
C_2	clearance due to inscribed circle on the bearing, mm
g	acceleration due to gravity, m s ⁻²
h_L	local fluid-film thickness
\bar{h}	nominal fluid-film thickness, (h/c)
\bar{h}_{TL}	average fluid-film thickness, (h_{TL}/c)
h_{min}	minimum fluid film thickness, mm
L	bearing length, mm
R_j, R_L, R_b	radius of journal, lobe and bearing, mm
r_c	radius of capillary, mm
d_o	orifice diameter, mm
p	pressure, N mm ⁻²
Q	bearing flow, mm ³ s ⁻¹
S_{ij}	stiffness coefficients ($i, j = X, Z$), N mm ⁻¹
C_{ij}	damping coefficients ($i, j = X, Z$), N s mm ⁻¹
$\lambda_{0.5x,y} = 0.5$	correlation lengths of the x and y profile, mm
t	time, s
ω_l	(g/c) ^{1/2} , rad s ⁻¹
D	journal diameter, mm
W_o	external load, N
μ	dynamic viscosity of lubricant, N s m ⁻²
ρ	density of lubricant, Kg mm ⁻³
z	combined roughness height, ($z = z_j + z_b$), μ m
z_j, z_b	roughness height in journal and bearing, μ m
σ	RMS value of combined roughness, $\sigma = (\sigma_j^2 + \sigma_b^2)^{1/2}$, μ m
σ_j	RMS value of journal surface roughness, μ m
σ_b	RMS value of bearing surface roughness, μ m
\bar{C}_{S2}	restrictor design parameter
erf	error function, $erf(x) = 2/\pi \int_0^x \exp(-y^2) dy$
n	number of rows of holes/slots
k	number of holes/slots per row
V_r	variance ratio
Y_s	radial length of slot, mm
Z_s	axial width of slot, mm
X, Y, Z	Cartesian coordinates
X_j, Z_j	coordinates of steady state equilibrium journal center from geometric center of bearing, mm
SOLV	program subroutine module used to solve modified system of equation
JECP	program subroutine module for equilibrium journal center position
SDPC	program subroutine module used to compute static and dynamic performance characteristics

Greek symbols

λ	aspect ratio
φ	altitude angle
O_j, O_{Li}	journal center, lobe center
ω_j	journal rotational speed, rad s ⁻¹
ω_{th}	threshold speed, rad s ⁻¹
p_s	lubricant supply pressure N mm ⁻²

Non-dimensional parameters

$\bar{a}_b = a_b/L$	land width ratio
$\beta^* = p^*/p_s$	concentric design pressure ratio
$\bar{C}_{ij} = C_{ij}(\bar{c}^3/\mu R_j^4)$	
$(\bar{F}, \bar{F}_o) = (F, F_o)/p_s R_j^2$	
$(\bar{h}) = (h)/c$	
$\bar{p}, \bar{p}_c, \bar{p}_{max} = (p, p_c, p_{max})/p_s$	
$\bar{C}_{S2} = \frac{1}{12}(\pi r_c^4/8c^3 l_c)$	for capillary restrictor
$\bar{C}_{S2} = \bar{Q}_c$	for constant flow valve restrictor
$\bar{C}_{S2} = \frac{1}{12}(3\pi d_o^2 \mu \psi_d/c^3)(2/\rho p_s)^{1/2}$	for orifice restrictor
$\psi_d =$	coefficient of discharge for orifice restrictor
$\bar{C}_{SR} = \frac{\pi}{36} \frac{SWR}{\lambda} \frac{k}{a_b} \frac{a_b}{Y_s} \left[\frac{Z_s}{c} \right]^3$	for slot restrictor
SWR	slot width ratio of a slot-entry bearing,
$SWR = \frac{a_s}{(a_s)_{max}} = \frac{a_s n}{\pi D}$	
$\bar{Q} = Q(\mu/c^3 p_s)$	
$\bar{Q}_{slot} = \frac{1}{12\eta}(\bar{p}_c - p) \frac{a_s Z_s^3}{Y_s}$	
$\bar{S}_{ij} = S_{ij}(c/p_s R_j^2)$	
$\bar{W}_o = W_o/p_s R_j^2$	
$\bar{z}, \bar{z}_j, \bar{z}_b = (z, z_j, z_b)/c$	
$(\bar{X}_j, \bar{Z}_j) = (X_j, Z_j)/c$	
$\bar{t} = t(c^2 p_s/\mu R_j^2)$	
$\bar{X}_L^i, \bar{Z}_L^i = (X_L^i, Z_L^i)/c$	
$\bar{V}_{rj}, \bar{V}_{rb} = ((\sigma_j, \sigma_b)/\sigma)^2$	
$\Lambda = c/\sigma$	surface roughness parameter
$\gamma = \lambda_{0.5x}/\lambda_{0.5y}$	surface pattern parameter
ϕ_{xL}, ϕ_{yL}	pressure flow factors
ϕ_{sL}	shear flow factor
ϕ_s	shear flow factor related to a single surface
$\alpha, \beta = (X, Y)/R_j$	circumferential and axial coordinates
$\varepsilon = e/c$	eccentricity ratio
$\delta = C_1/C_2$	offset factor
$\bar{\omega}_{th} = \omega_{th}/\omega_l$	
$\Omega = \omega_j \mu R_j^2/c^2 p_s$	Speed parameter

Matrices

$N_i, N_j =$	shape functions
$[\bar{F}]$	assembled fluidity matrix
$\{\bar{p}\}$	nodal pressure vector
$\{\bar{Q}\}$	nodal flow vector
$\{\bar{R}_H\}$	column vectors due to hydrodynamic terms
$\{\bar{R}_{X_j}\}, \{\bar{R}_{Z_j}\}$	global right hand side vector due to journal center velocities.

Subscripts and superscripts

b	bearing
J	journal
R	restrictor
s	supply
l	lobe
i	lobe number
min	minimum
max	maximum
x, y, z	components in X, Y, and Z directions
.	first derivative w.r.t time
r	reference value
*	concentric operation
..	second derivative w.r.t time
—	non-dimensional parameter

A theoretical investigation, accounting the influence of bearing surface damage due to wear on the performance of a 2-lobe 4-pocket hybrid journal bearing employed with different flow restrictors was presented by Phalle et al. [5]. Further, Sharma et al. [21] investigated the influence of misalignment and wear on the performance of three lobe three pocket hybrid journal bearing. The findings of their studies [5,21] opined that wear has a quite substantial influence on the performance of the bearing system. The main feature of the above studies was that these were limited to only recessed hybrid journal bearings. Very few studies are available in the open literature that concerns with the multilobe non-recessed hybrid journal bearings [22–24]. Recently, an analytical study referring to a misaligned rough lobed hole-entry (symmetric-24 holes) hybrid journal bearing was carried out by Basavaraja et al. [22]. Kushare and Sharma [23] carried out an analytical study on the effect of wear defect on the performance of two lobe hole entry hybrid bearing system compensated with orifice restrictor, lubricated with non-Newtonian lubricant. Further, they [24] studied the stability of non-linear journal motion for two lobe symmetric hole entry worn hybrid journal bearing operating with non-Newtonian lubricant. They [23,24] reported that the non-linear behavior of lubricant and wear defect deteriorates the bearing performance and its stability.

In the design of bearing system, many researchers and investigators [9,11,13,15,23–24] have presumed that journal and bearing surfaces are smooth. Due to the technological advancement in manufacturing processes; fabrication of precise bearing surfaces have become possible, but still the surface roughness exist at microscopic scale. Under this state of affairs, an analysis based upon the premise of a smooth surface does not give a pragmatic bearing performance. In reality, rough surface with a multitude of hills and valleys, prevent the surface contact and support in maintaining the lubricating film. In many of the cases, roughness of the bearing surface is of the same order of magnitude as that of the fluid-film thickness. As a result of this, bearing performance gets affected. So, for correct prediction of bearing performance characteristics, consideration of surface roughness is highly imperative.

In recent years, many studies concerning the influence of surface roughness on the performance characteristics of hydrodynamic journal bearings [25–28,30–33] and circular hydrostatic/hybrid journal bearings [4,6,22,35–36] have been reported in the literature. Christensen and Tonder [26] developed and applied stochastic model for random rough surface and investigated the influence of longitudinal and transverse roughness on the performance characteristics of journal bearing. The average flow model developed by Patir and Cheng [28,29] have been exhaustively used by many researchers [4,6,22,30–33,36]. Ramesh et al. [30] carried out thermo hydrodynamic analysis of rough bearing using Patir and Cheng [28] average flow model. San Andres [34] carried out theoretical investigations on recessed hybrid journal bearing by varying the effective depth of roughness. An experimental study on the influence of round-hole-pattern roughness on performance characteristics of a hybrid journal bearing system has been reported by Fayolle and Childs [35]. Further, Nagaraju et al. [4] carried out a theoretical study on the influence of surface roughness parameter on the performance of circular hole entry journal bearing and extended this work [6,36] to study the combined influence of roughness, bearing flexibility and thermal effects. The result of these studies [6,36] shows significant improvement in bearing performance characteristics. The studies available in literature corresponding to the influence of roughness are mainly confined to hydrodynamic journal bearing and circular recessed and non-recessed hybrid journal bearings except the study by Basavraj et al. [22]. The study carried by Basavraj et al. [22] is not comprehensive one and is only limited to capillary compensated symmetric bearing configuration.

A thorough scan of the literature, which deals with the studies related to the influence of surface roughness pattern on the performance of non-circular non-recessed hybrid journal bearing, reveals that there is very limited information available on these class of bearings. A proper selection of flow control device may have a significant role in the overall performance of the bearing. However, till date, no study has yet been reported concerning the influence of surface roughness on the performance of two lobe non-recessed hybrid journal bearing compensated with different restrictors. Therefore, the objective of this paper is to evaluate the influence of surface roughness on the performance of two lobe symmetric non-recessed hybrid journal bearings compensated with orifice, capillary, constant flow valve and slot entry restrictors.

2. Analysis

The modified Reynold's equation governing the laminar flow of isoviscous lubricant for two lobe non-recessed hybrid journal bearing system with rough surfaces as shown in Fig. 1(a,b) in the non-dimensional form can be written as [4,6,8,22,28–30,36]

$$\frac{\partial}{\partial \alpha} \left(\phi_{xL} \frac{\bar{h}^3}{12} \frac{\partial \bar{p}}{\partial \alpha} \right) + \frac{\partial}{\partial \beta} \left(\phi_{yL} \frac{\bar{h}^3}{12} \frac{\partial \bar{p}}{\partial \beta} \right) = \frac{\Omega}{2} \frac{\partial \bar{h}_{TL}}{\partial \alpha} + \frac{\Omega}{2\Lambda} \frac{\partial \phi_{sL}}{\partial \alpha} + \frac{\partial \bar{h}_{TL}}{\partial \tau} \quad (1)$$

where ϕ_{xL}, ϕ_{yL} are the pressure flow factors and expressed as [28,30,33]

$$\phi_{xL} = 1 - Ce^{-r\Lambda\bar{h}} \quad \text{for } \gamma \leq 1 \quad (1a)$$

$$\phi_{xL} = 1 + C(\Lambda\bar{h})^{-r} \quad \text{for } \gamma > 1 \quad (1b)$$

$$\phi_{yL}(\Lambda\bar{h}, \gamma) = \phi_{xL}(\Lambda\bar{h}, 1/\gamma) \quad (1c)$$

The shear flow factor ϕ_{sL} represents the additional flow of lubricant along the circumferential direction due to rotation of the journal. The shear flow factor ϕ_{sL} is a function of nominal fluid-film thickness \bar{h} and surface roughness parameter Λ only. For same roughness pattern (i.e. $\gamma_j = \gamma_b = \gamma$), of bearing and journal, the shear flow factor in non-dimensional form is expressed as [29]

$$\phi_{sL} = (\bar{V}_{rj} - \bar{V}_{rb}) \Phi_s(\Lambda\bar{h}, \gamma)$$

$$\phi_{sL} = (2\bar{V}_{rj} - 1) \Phi_s(\Lambda\bar{h}, \gamma) \quad (1d)$$

The shear flow factor Φ_s is a positive function of \bar{h}/σ and γ of an individual surface and is expressed as [29]

$$\Phi_s = A_1 (\Lambda\bar{h})^{\alpha_1} \exp^{-\alpha_2 (\Lambda\bar{h}) + \alpha_3 (\Lambda\bar{h})^2} \quad \text{for } \Lambda\bar{h} \leq 5.0 \quad (1e)$$

$$\Phi_s = A_2 \exp^{-0.25 (\Lambda\bar{h})} \quad \text{for } \Lambda\bar{h} > 5.0 \quad (1f)$$

where $C, r, A_1, A_2, \alpha_1, \alpha_2$ and α_3 are constants [28,29].

The directional properties of surface roughness orientation can be accounted in the analysis using surface pattern parameter (γ) defined as

$$\gamma = \lambda_{0.5x} / \lambda_{0.5y} \quad (1g)$$

where $\lambda_{0.5x}$ and $\lambda_{0.5y}$ are the autocorrelation lengths of x profile and y profile. The surface pattern parameter (γ) can be interpreted as the length to width ratio of a representative asperity. Practically, the surface topography can be measured using advanced mechanical, optical or electrical probes, which tells the presence of high frequency component of surface roughness. Further, by using the optical profilometer, asperity inherited with random roughness is presented in profile form. The statistical analysis of the random surface roughness provides the data of autocorrelation lengths of x profile and y profile.

When the pressure flow factors $\phi_{xL}, \phi_{yL} \rightarrow 1$ and shear flow factor $\phi_{sL} \rightarrow 0$, Eq. (1) becomes Reynold's equation for smooth

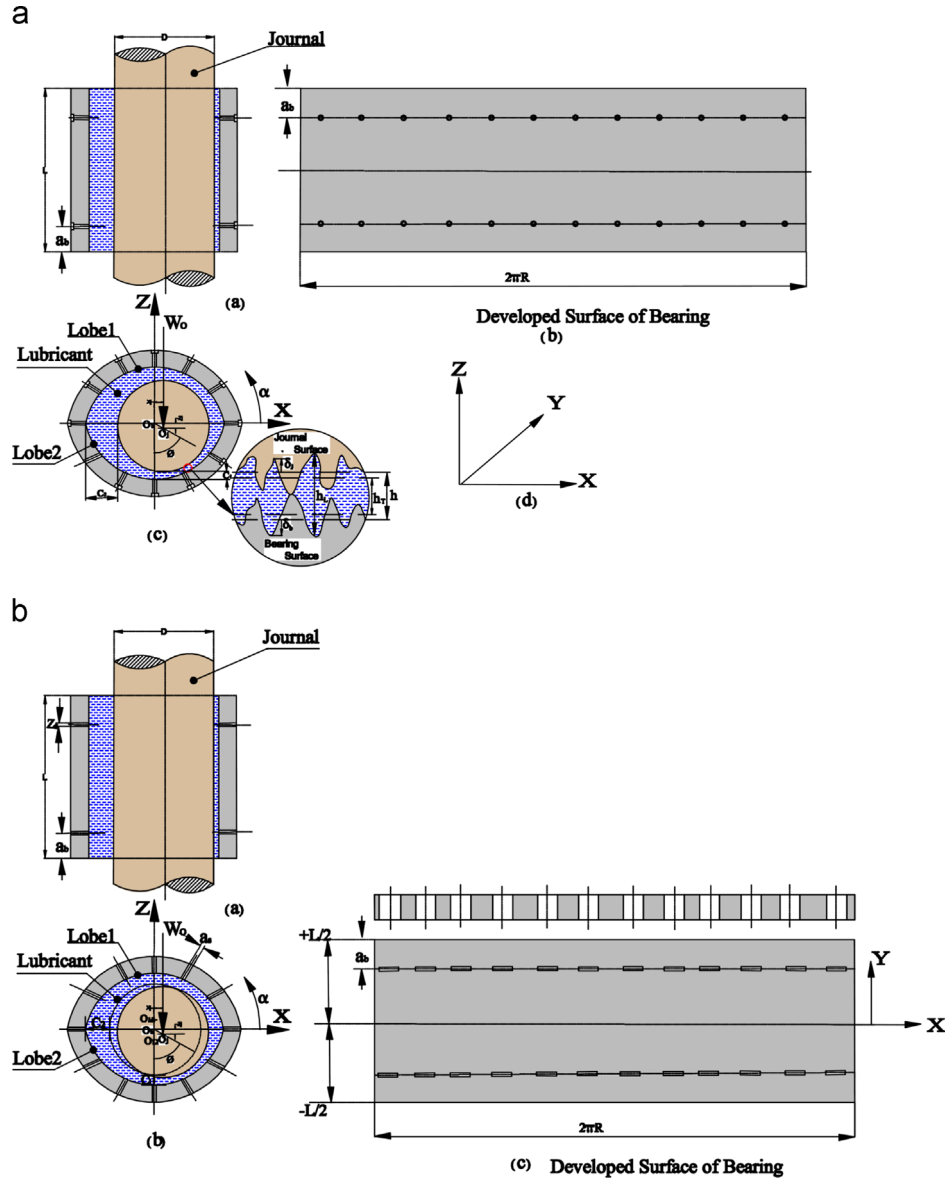


Fig. 1. (a) Two lobe symmetric hole entry journal bearing system and (b) Two lobe symmetric slot entry journal bearing system.

bearing. The modified Reynold's Eq. (1) has been solved by using the finite element methods. The lubricant flow field in the clearance space of two lobe non-recessed hybrid journal bearing has been discretized using a four-noded isoparametric element. Further, Galerkin's orthogonality condition is employed to yield the elemental system of equation in the matrix form as [20,24,36]

$$[\bar{F}] \{ \bar{p} \} = \{ \bar{Q} \} + \Omega \{ \bar{R}_H \} + \bar{X}_J \{ \bar{R}_{xj} \} + \bar{Z}_J \{ \bar{R}_{zj} \} \quad (2)$$

2.1. Average fluid-film thickness (\bar{h}_{TL})

The expression for multilobe journal bearing in the non-dimensional form is written as [17,18,20,23]

$$\bar{h} = \frac{1}{\delta} - (\bar{X}_J + \bar{x} - \bar{X}_L^i) \cos \alpha - (\bar{Z}_J + \bar{z} - \bar{Z}_L^i) \sin \alpha \quad (3)$$

The average fluid-film thickness (\bar{h}_{TL}) is written as [37]

$$\bar{h}_{TL} = E[\bar{h} + \bar{\delta}] = \int_{-\infty}^{\infty} (\bar{h} + \bar{\delta}) \psi(\bar{\delta}) d\bar{\delta} \quad (4)$$

where $\psi(\bar{\delta})$ is the probability density function for combined roughness $\bar{\delta}$ and is expressed as

$$\psi(\bar{\delta}) = \frac{1}{\sqrt{2\pi}\bar{\sigma}} e^{-\bar{\delta}^2/2\bar{\sigma}^2} \quad (4a)$$

$\bar{\sigma}$ is the combined rms or standard deviation of roughness and is expressed as

$$\bar{\sigma} = (\bar{\sigma}_f^2 + \bar{\sigma}_b^2)^{1/2} \quad (4b)$$

For a mixed lubrication regime of the bearing (i.e. $\Lambda\bar{h} < 3$), the maximum projection of distance of surface asperities into the fluid film is equal to the nominal fluid-film thickness \bar{h} . Applying this condition to Eq. (4), the average fluid-film thickness for mixed lubrication regime can be written as [4,22,30]

$$\bar{h}_{TL} = \frac{\bar{h}}{2} \left(1 + \operatorname{erf} \left(\frac{\Lambda\bar{h}}{\sqrt{2}} \right) \right) + \frac{1}{\Lambda\sqrt{2\pi}} e^{-(\Lambda\bar{h})^2/2} \quad \text{for } \Lambda\bar{h} < 3 \quad (4c)$$

For full lubrication regime, since \bar{h} is constant for a given value of circumferential coordinate

(α), the expected value of \bar{h} becomes [6]

$$E[\bar{h}] = \bar{h} \int_{-\infty}^{\infty} \psi(\bar{\delta}) d\bar{\delta}$$

$$E[\bar{h}] = \bar{h} \text{ as } \int_{-\infty}^{\infty} \psi(\bar{\delta}) d\bar{\delta} = 1 \quad (4d)$$

Further, since $\bar{\delta}$ is a random variable with mean zero, the expected value of $\bar{\delta}$ in fully lubricated regime becomes equal to zero (i.e. $E[\bar{\delta}] = 0$).

Then the non-dimensional form of an average fluid-film thickness is expressed as [36,37]

$$\bar{h}_{TL} = \bar{h} \text{ for } \Lambda \bar{h} \geq 3. \quad (4e)$$

2.2. Restrictor flow equations

The lubricant flow through various compensating devices in the non-dimensional form is expressed as [1,3,5]

$$\bar{Q}_R = \bar{C}_{s2}(1 - \bar{p}_c) \text{ Capillary} \quad (5a)$$

$$\bar{Q}_R = \bar{C}_{s2}(1 - \bar{p}_c)^{1/2} \text{ Orifice} \quad (5b)$$

$$\bar{Q}_R = \bar{Q}_c \text{ Constant flow valve} \quad (5c)$$

$$\bar{Q}_R = \bar{C}_{SR}(1 - \bar{p}_c) \text{ Slot.} \quad (5d)$$

2.3. Boundary conditions

To establish the lubricant flow field, following boundary conditions have been used [1,3,23,36]:

- 1 All the nodes situated on holes/slots have equal pressure.
- 2 Flow of lubricant through the restrictor is equal to the bearing input flow at hole and slot.
- 3 Nodes situated on the external boundary of the bearing have zero pressure. $\bar{p}|_{\beta = \mp 1.0} = 0.0$.
- 4 At the trailing edge of the positive region.

$$\bar{p} = \frac{\partial \bar{p}}{\partial \alpha} = 0.0 \text{ Reynold's boundary condition.}$$

In the present work the holes/slots are assumed to be quite deep, this assumption makes that the pressure within the holes/slots remain uniform. Further, the fluidity matrix corresponding to each restrictor equation needs to be adjusted accordingly in order to maintain the continuity of flow [1,3]. To satisfy the boundary condition (1) of equal pressure on nodes situated at all the holes/slots. The elemental system Eq. (2) is adjusted for a single unknown pressure and a single unknown flow to each hole/slot. By using restrictor parameters, the hole/slot flow can be obtained. This unknown hole/slot flow is equated to restrictor flow, which is given by Eqs. (5a)–(5d). To keep the number of iterations small, the initial trial solution from the respective flow control device is used to obtain the nodal pressures and bearing flows.

2.4. Dynamic fluid film coefficients

2.4.1. Fluid-film stiffness coefficients

The fluid-film stiffness coefficients are expressed as [20,23,36]

$$\bar{S}_{ij} = -\frac{\partial \bar{F}_i}{\partial q_j} (i = x, z) \quad (6)$$

where 'i' represents the direction of force and $q_j = \bar{X}_j, \bar{Z}_j$.

Stiffness coefficient in matrix form can be written as

$$\begin{bmatrix} \bar{S}_{xx} & \bar{S}_{xz} \\ \bar{S}_{zx} & \bar{S}_{zz} \end{bmatrix} = - \begin{bmatrix} \frac{\partial \bar{F}_x}{\partial \bar{X}_j} & \frac{\partial \bar{F}_x}{\partial \bar{Z}_j} \\ \frac{\partial \bar{F}_z}{\partial \bar{X}_j} & \frac{\partial \bar{F}_z}{\partial \bar{Z}_j} \end{bmatrix} \quad (6a)$$

$$\begin{bmatrix} \bar{S}_{xx} & \bar{S}_{xz} \\ \bar{S}_{zx} & \bar{S}_{zz} \end{bmatrix} = \begin{bmatrix} -\frac{\partial}{\partial \bar{X}_j} \int_{-\lambda}^{\lambda} \int_0^{2\pi} \bar{p} \cos \alpha d\alpha d\beta & -\frac{\partial}{\partial \bar{Z}_j} \int_{-\lambda}^{\lambda} \int_0^{2\pi} \bar{p} \cos \alpha d\alpha d\beta \\ -\frac{\partial}{\partial \bar{X}_j} \int_{-\lambda}^{\lambda} \int_0^{2\pi} \bar{p} \sin \alpha d\alpha d\beta & -\frac{\partial}{\partial \bar{Z}_j} \int_{-\lambda}^{\lambda} \int_0^{2\pi} \bar{p} \sin \alpha d\alpha d\beta \end{bmatrix} \quad (6b)$$

2.4.2. Fluid-film damping coefficients

The fluid-film damping coefficients are expressed as [20,23,36]

$$\bar{C}_{ij} = -\frac{\partial \bar{F}_i}{\partial \dot{q}_j} (i = x, z) \quad (7)$$

\dot{q}_j represents the velocity component of journal center and is expressed as $\dot{q}_j = \dot{\bar{X}}_j$ or $\dot{\bar{Z}}_j$.

In matrix form, damping coefficients are expressed as

$$\begin{bmatrix} \bar{C}_{xx} & \bar{C}_{xz} \\ \bar{C}_{zx} & \bar{C}_{zz} \end{bmatrix} = - \begin{bmatrix} \frac{\partial \bar{F}_x}{\partial \dot{\bar{X}}_j} & \frac{\partial \bar{F}_x}{\partial \dot{\bar{Z}}_j} \\ \frac{\partial \bar{F}_z}{\partial \dot{\bar{X}}_j} & \frac{\partial \bar{F}_z}{\partial \dot{\bar{Z}}_j} \end{bmatrix} \quad (7a)$$

$$\begin{bmatrix} \bar{C}_{xx} & \bar{C}_{xz} \\ \bar{C}_{zx} & \bar{C}_{zz} \end{bmatrix} = \begin{bmatrix} -\frac{\partial}{\partial \dot{\bar{X}}_j} \int_{-\lambda}^{\lambda} \int_0^{2\pi} \bar{p} \cos \alpha d\alpha d\beta & -\frac{\partial}{\partial \dot{\bar{Z}}_j} \int_{-\lambda}^{\lambda} \int_0^{2\pi} \bar{p} \cos \alpha d\alpha d\beta \\ -\frac{\partial}{\partial \dot{\bar{X}}_j} \int_{-\lambda}^{\lambda} \int_0^{2\pi} \bar{p} \sin \alpha d\alpha d\beta & -\frac{\partial}{\partial \dot{\bar{Z}}_j} \int_{-\lambda}^{\lambda} \int_0^{2\pi} \bar{p} \sin \alpha d\alpha d\beta \end{bmatrix} \quad (7b)$$

3. Solution scheme

The solution for the problem to investigate the influence of surface roughness on the performance of a two lobe non-recessed hybrid journal bearing system is obtained by using iterative scheme. Reynolds equation (Eq. (1)) and the restrictor flow equations (Eqs. (5a)–(5d)) are solved together with appropriate boundary conditions (Section 2.3) to get the simultaneous solution. The overall solution scheme shown in Fig. 2 is employed for obtaining the solution and has been explicated in the subsequent steps:

1. The geometric and operating data along with 2D mesh data is read in Unit PDATA.

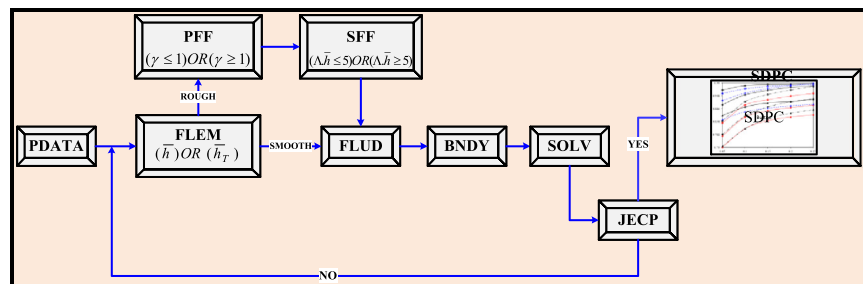


Fig. 2. Overall solution scheme.

- Assuming steady state condition, unit FLEM computes the value of nominal fluid film thickness for the given eccentricity ratio and then also calculates the value of average fluid film thickness (\bar{h}_{TL}) at all the nodal points by using Eqs. (4c) and (4e).
- In unit PPF and SFF, pressure flow factors (ϕ_{xL} , ϕ_{yL}) and shear flow factor (ϕ_{sL}) are calculated using Eqs. (1a), (1c) and (1d) respectively.
- The elemental fluidity system equation expressed by Eq. (2) are generated and assembled in unit FLUD.
- The system equation (Eq. (2)) and the restrictor flow equations (Eqs. (5a)–(5d)) are solved together with apposite boundary conditions to get nodal values of fluid film pressure.
- The unit BNDY modify the system of equations for apposite boundary conditions and the modified system of equation is directly solved for the nodal pressure in the unit SOLV using Newton–Raphson iterative method for orifice restrictor and Gaussian elimination technique for the capillary and CFV restrictor to get the values of pressure corrections.
- To obtain a solution for a specified value of external load, the equilibrium journal center position is attained in unit JECF.
- The iterative process is repeated until the convergence is achieved. When equilibrium the journal center position is achieved, the performance characteristics of lobed non-recessed hybrid journal bearing system are computed in unit SDPC.

4. Result and discussion

Using the analysis and solution scheme as described in the previous section, the influence of surface roughness on the performance characteristics of a two lobe non-recessed hybrid journal bearing compensated with orifice, capillary, constant flow valve and slot restrictor have been obtained. As stated earlier, no studies concerning the influence of roughness on the performance of a two lobe non-recessed hybrid journal bearing compensated with different restrictors is available in the published literature. Therefore, to ascertain the validity of developed numeric model, the computed results have been validated and compared with the earlier published results of Rowe et al. [1] and Ramesh et al. [30] for the case of symmetric circular hole and slot entry hydrostatic journal bearing and surface roughness respectively. At the onset, for symmetric circular hole and slot entry smooth surface hydrostatic journal bearing systems, the results have been computed for a journal bearing compensated with orifice, capillary and slot restrictor and compared with the published results of Rowe et al. [1] as shown in Fig. 3. These results agree quite well with a maximum deviation of 7–7.5% at higher eccentricity ratio. Further, the results for both the plain smooth and rough hydrodynamic journal bearing is computed. The results show better agreement when compared with the published results of Ramesh et al. [30] as shown in Fig. 4. The deviation observed between the two results may be attributed to the different numerical techniques used. The values of bearing operating and geometric parameters as shown in Table 1 have been used to simulate the results numerically. The parameters used in the present study are taken from the already published literature [1–6,17–19,27–30,33 and 38] on the basis of their wide applications.

The static and dynamic bearing performance characteristics have been computed for different values of surface roughness pattern parameter (γ). The value of roughness pattern parameter depends upon the roughness orientation. In transversely oriented roughness pattern, the 0.5 autocorrelation length of a profile in axial direction is greater than the circumferential direction (i.e. $\lambda_{0.5y} > \lambda_{0.5x}$) and hence the value of the surface pattern parameter γ becomes less than one ($\gamma < 1$). In isotropic pattern, the roughness is uniformly distributed over the bearing surface

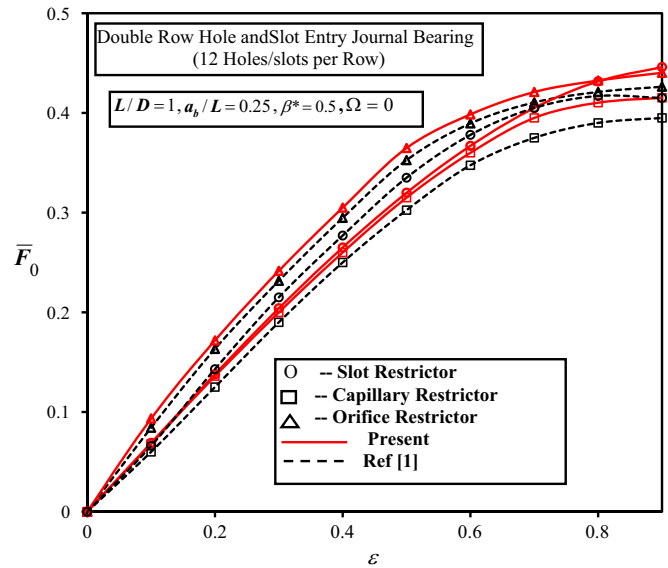


Fig. 3. Fluid film reaction (\bar{F}_0) with eccentricity ratio (ϵ).

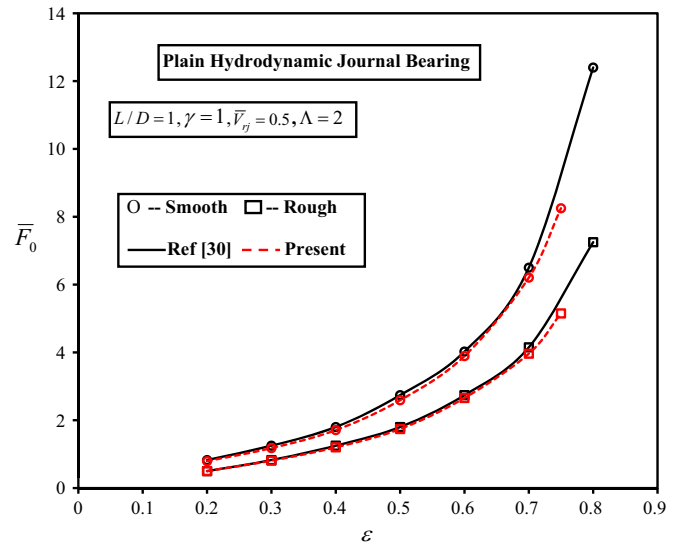


Fig. 4. Fluid film reaction (\bar{F}_0) with an eccentricity ratio (ϵ).

with no preferred direction or position. The size of the asperities in both axial and circumferential direction is assumed to be same (i.e. $\lambda_{0.5x} = \lambda_{0.5y}$). Therefore, the values of surface pattern parameter $\gamma = 1$ for this isotropic pattern. In longitudinally oriented roughness pattern, the 0.5 autocorrelation length along the circumferential direction is greater than that of axial direction (i.e. $\lambda_{0.5x} > \lambda_{0.5y}$) and hence the values of surface pattern parameter γ for this pattern become more than one (i.e. $\gamma > 1$).

The influence of surface roughness and the offset factor on the performance of a two lobe symmetric non-recessed hybrid journal bearing system have been investigated for different restrictors such as an orifice, capillary, CFV and slot. The bearing performance characteristics viz. \bar{P}_{max} , \bar{h}_{min} , \bar{Q} , \bar{S}_{11} , \bar{S}_{22} , \bar{C}_{11} , \bar{C}_{22} and $\bar{\omega}_{th}$ have been computed as a function of an external load (\bar{W}_0). To be concise, these results have been presented in detail for orifice compensated two lobe symmetric non-recessed hybrid journal bearings as shown in Figs. 5–12.

4.1. Influence on maximum fluid film pressure (\bar{P}_{max})

Fig. 5(a) shows the variation of maximum fluid film pressure (\bar{P}_{max}) for a two lobe symmetric bearing system. From Fig. 5(a),

Table 1
Geometric and operating parameters of bearing [1–6,17–19,27–30,33 and 38].

Operating parameters		Geometric parameters	
Parameters	Value/Range	Parameters	Value
External load (\bar{W}_0)	1.0–1.4	Aspect ratio (λ)	1.0
Symmetric bearing configuration		No. of holes/slots per row (k)	12
Compensating elements	Orifice Capillary CFV Slot	No. of rows (n)	02
		Land width ratio (\bar{a}_b)	0.25
Surface roughness parameter (λ)	4		
Surface pattern parameter (γ)	1/6, 1 and 6	Clearance ratio (\bar{c})	0.001
Variance ratio (\bar{V}_{ff})	0.5		
Speed parameter (Ω)	1.0	Concentric design pressure ratio (β^*)	0.5
Offset factor (δ)	0.9, 1.0 and 1.1		

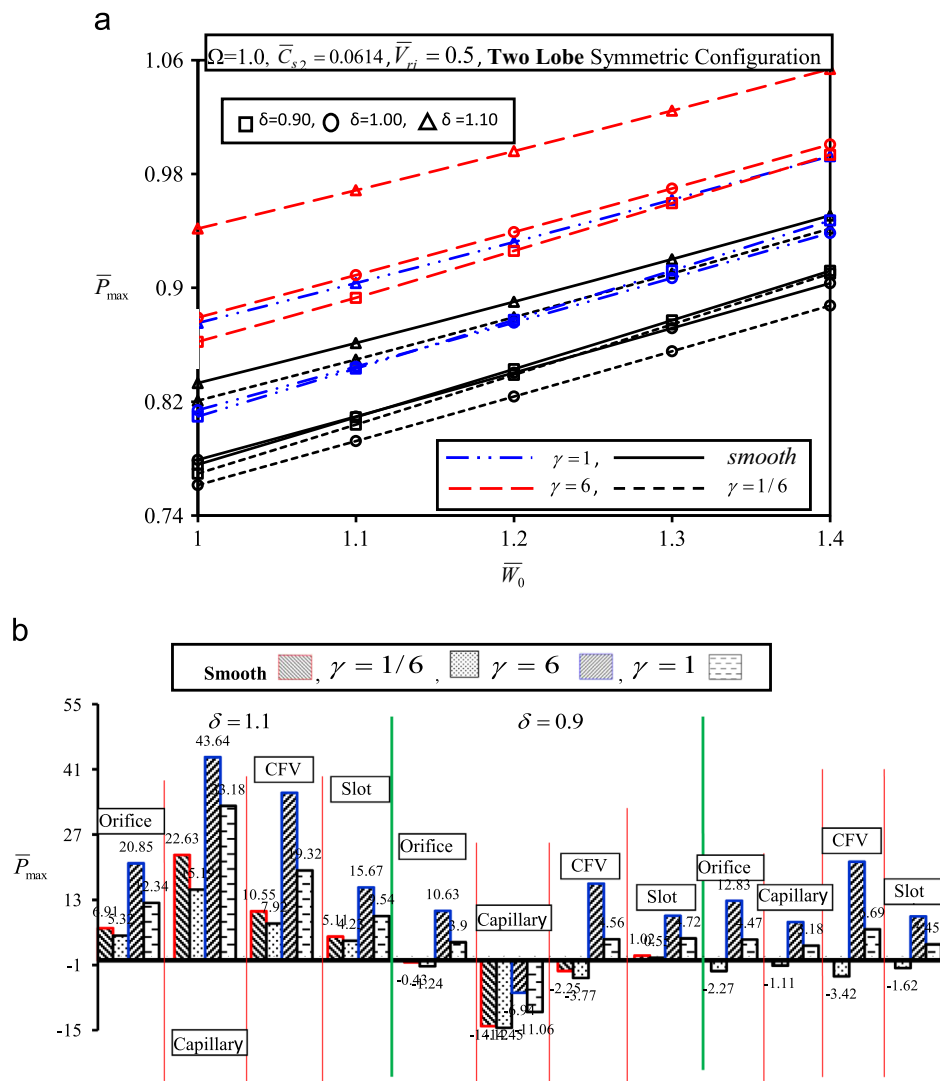


Fig. 5. (a) Variation of \bar{P}_{max} for symmetric two lobe journal bearing and (b) Percentage change in \bar{P}_{max} w.r.t base bearing for symmetric two lobe journal bearing ($\bar{W}_0 = 1.0$).

it has been observed that circular bearing with smooth and transverse surface orientation operates at lower values of pressure, whereas; the bearing with longitudinal surface orientation operates at higher values of maximum pressure than isotropic and the transverse surface roughness pattern at offset factor $\delta = 0.9, 1.0$ and 1.1 . Fig. 5(b) indicates the % change in \bar{P}_{max} w.r.t base bearing. At a constant value of external load ($\bar{W}_0 = 1.0$); it has been

observed that a bearing compensated with capillary restrictor provides a higher value of \bar{P}_{max} as compared to orifice, CFV and slot restrictor bearing when bearing operates at offset factor $\delta > 1.1$. This is due to the resistance offered by the capillary restrictor geometry. For a given load ($\bar{W}_0 = 1.0$), flow through the capillary restrictor get decreased as the film thickness decreases. A low value of pressure at hole point outs a large flow resistance through the

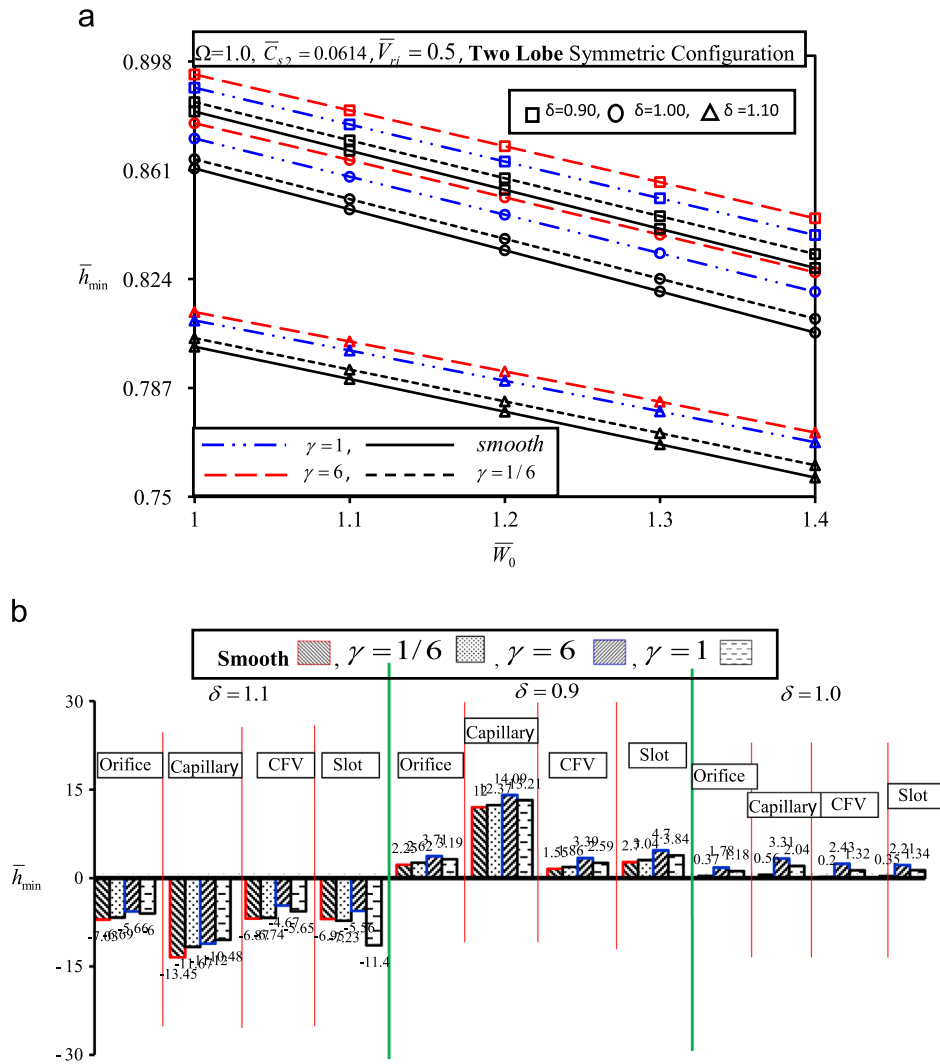


Fig. 6. (a) Variation of \bar{h}_{min} for symmetric two lobe journal bearing and (b) Percentage change in \bar{h}_{min} w.r.t base bearing for symmetric two lobe journal bearing ($\bar{W}_0 = 1.0$).

restrictor, whereas a large pressure at hole indicates a large flow resistance through the film lands. Thus, an increased eccentricity provides a more convergent section at the bottom of the bearing. Therefore, fluid film pressure gets increased and bearing operates at higher value of \bar{P}_{max} when compared with other restrictors. The bearing with the transverse surface roughness pattern operates at lower values of maximum fluid pressure \bar{P}_{max} for all compensating devices. The percentage change in the value of \bar{P}_{max} corresponding to the transverse pattern has been observed to the order of 20.85%, 43.64%, 36% and 15.67% respectively for the orifice, capillary, CFV and slot restrictor vis-à-vis smooth surface circular journal bearing. Therefore, in order to attain a higher value of \bar{P}_{max} for all roughness patterns, capillary compensated bearing with offset factor $\delta > 1.1$ is found to be more suitable than the other compensating devices.

4.2. Influence on minimum fluid film thickness (\bar{h}_{min})

The variation of fluid film thickness (\bar{h}_{min}) is shown in Fig. 6 (a) as a function of external load for orifice compensated two lobe journal bearing. From Fig. 6(a), it is observed that bearing with smooth surface and offset factor ($\delta = 1.1$) operates at lower values of minimum fluid film thickness. As the surface becomes rough, the value of \bar{h}_{min} for circular ($\delta = 1.0$) and non-circular journal bearing is observed to increase. Further, it may be observed that the longitudinal roughness pattern ($\gamma = 6$) helps in enhancing the

value of minimum fluid film thickness over the transverse ($\gamma = 1/6$) and isotropic surface pattern ($\gamma = 1$). This is due to the fact that, the longitudinal surface has larger correlation length in the direction of flow and it does not permit much side flow in axial direction. Further, the transverse roughness pattern increases the resistance to circumferential flow, thereby decreasing the values of minimum fluid film thickness. Hence the bearing operates at lower values of minimum fluid film thickness (\bar{h}_{min}). Due to the change in bearing geometry, the bearing with offset factor $\delta = 0.9$, operates at higher value of minimum fluid film thickness.

For the chosen values of external load ($\bar{W}_0 = 1.0$), restrictor design parameter (\bar{C}_{s2}), surface roughness parameter $\Lambda = 4.0$ and offset factor $\delta = 1.1$, the capillary compensated two lobe journal bearing with transverse ($\gamma = 1/6$) roughness pattern provides a lower value of \bar{h}_{min} as compared to constant flow valve, orifice and slot entry restrictor. This is because of the 0.5 autocorrelation length of a profile in axial direction is greater than the circumferential direction for transverse roughness pattern ($\gamma = 1/6$). It increases the resistance to circumferential flow. Further, external load acting on the bearing reduces the value of \bar{h}_{min} . Thus, for the decreased value of \bar{h}_{min} , capillary compensation becomes less stiff through decreased flow from capillary restrictor than orifice fed. As shown in Fig. 6(b), the percentage reduction in the value of minimum fluid film thickness (\bar{h}_{min}) due to roughness pattern $\gamma = 1/6$ and offset factor $\delta = 1.1$ is found to be of the order of

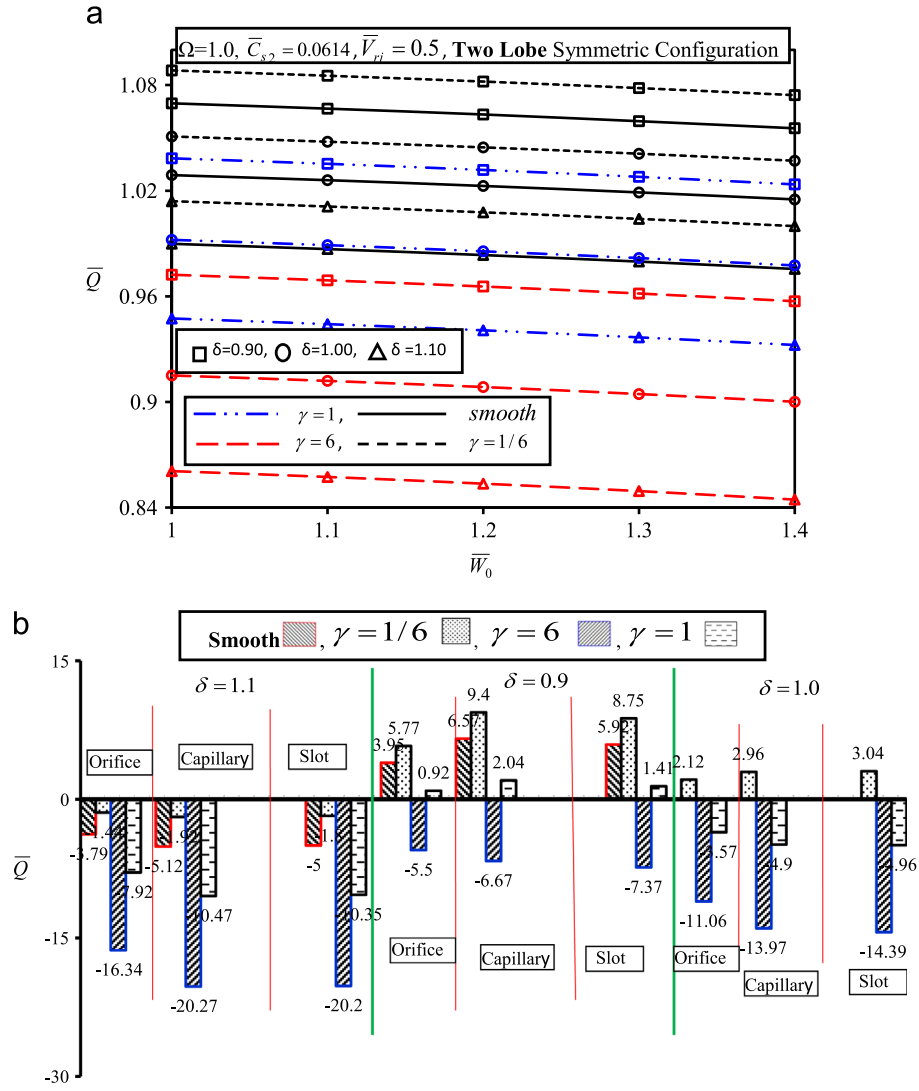


Fig. 7. (a) Variation of \bar{Q} for symmetric two lobe journal bearing. (b) Percentage change in \bar{Q} w.r.t base bearing for symmetric two lobe journal bearing ($\bar{W}_0 = 1.0$).

11.67%, 7.23%, 6.74% and 6.69% respectively for capillary, slot entry, constant flow valve and orifice compensated bearings with respect to smooth circular non-recessed journal bearing system. Further, for the higher values of external load ($\bar{W}_0 = 1.4$), offset factor $\delta = 1.1$ and $\gamma = 1/6$, the maximum reduction in the value of \bar{h}_{\min} is observed to the order of 4–6% for all compensating devices. The slot entry bearing with isotropic and transverse surface roughness pattern provides lower values of minimum fluid film thickness than the smooth bearings. This can be attributed to the increase in shear flow factors due to slot positions. It has been observed that the offset factors greater than one have a significant effect on the minimum fluid film thickness and the bearing operates at lower values of \bar{h}_{\min} . At a constant value of external load $\bar{W}_0 = 1.0$ and $\delta = 1.1$, the value of \bar{h}_{\min} increases for isotropic surface roughness pattern when bearings are compensated with capillary and CFV restrictor. The maximum reduction in the value of \bar{h}_{\min} is observed to the order of 7–8% for all flow controlling devices. As noticed from Fig. 6(a,b), the bearing with offset factor $\delta = 1.1$, runs at a lower value of minimum film thickness. Therefore, for safe bearing operation, proper selection of roughness patterns, offset factor and proper compensating device is essential to maintain the required value of minimum fluid film thickness (\bar{h}_{\min}). The designer may use the following criterion for the selection of appropriate restrictors.

For orifice, CFV restrictors at $\delta = 1.1$, $\bar{h}_{\min}|_{\text{smooth}} < \bar{h}_{\min}|_{\gamma=1/6} < \bar{h}_{\min}|_{\gamma=1.0} < \bar{h}_{\min}|_{\gamma=6}$.
 For capillary restrictor with $\delta = 1.1$, $\bar{h}_{\min}|_{\text{smooth}} < \bar{h}_{\min}|_{\gamma=1/6} < \bar{h}_{\min}|_{\gamma=6} < \bar{h}_{\min}|_{\gamma=1.0}$.
 For slot restrictor with $\delta = 1.1$, $\bar{h}_{\min}|_{\gamma=1.0} < \bar{h}_{\min}|_{\gamma=1/6} < \bar{h}_{\min}|_{\text{smooth}} < \bar{h}_{\min}|_{\gamma=6}$.

4.3. Influence on bearing flow (\bar{Q})

Fig. 7(a) shows the effect of surface roughness orientations (γ) on bearing flow (\bar{Q}) in two lobe non-recessed hybrid journal bearing. The isotropic ($\gamma = 1$) and longitudinal ($\gamma = 6$) roughness patterns reduce the supply of bearing flow (\bar{Q}). Since the longitudinal ($\gamma = 6$) roughness pattern has asperities with long correlation length in the circumferential direction (i.e. $\gamma = \lambda_{0.5x}/\lambda_{0.5y} > 1$). It provides resistance to the bearing flow and hence reduction in bearing flow is more for the longitudinal roughness pattern. Whereas, the transverse roughness pattern ($\gamma = \lambda_{0.5x}/\lambda_{0.5y} < 1$) has long correlation length in axial direction it enhances the bearing flow (side leakage). From Fig. 7(a), it can be seen that the bearing flow is reduces with an increase in the value of offset

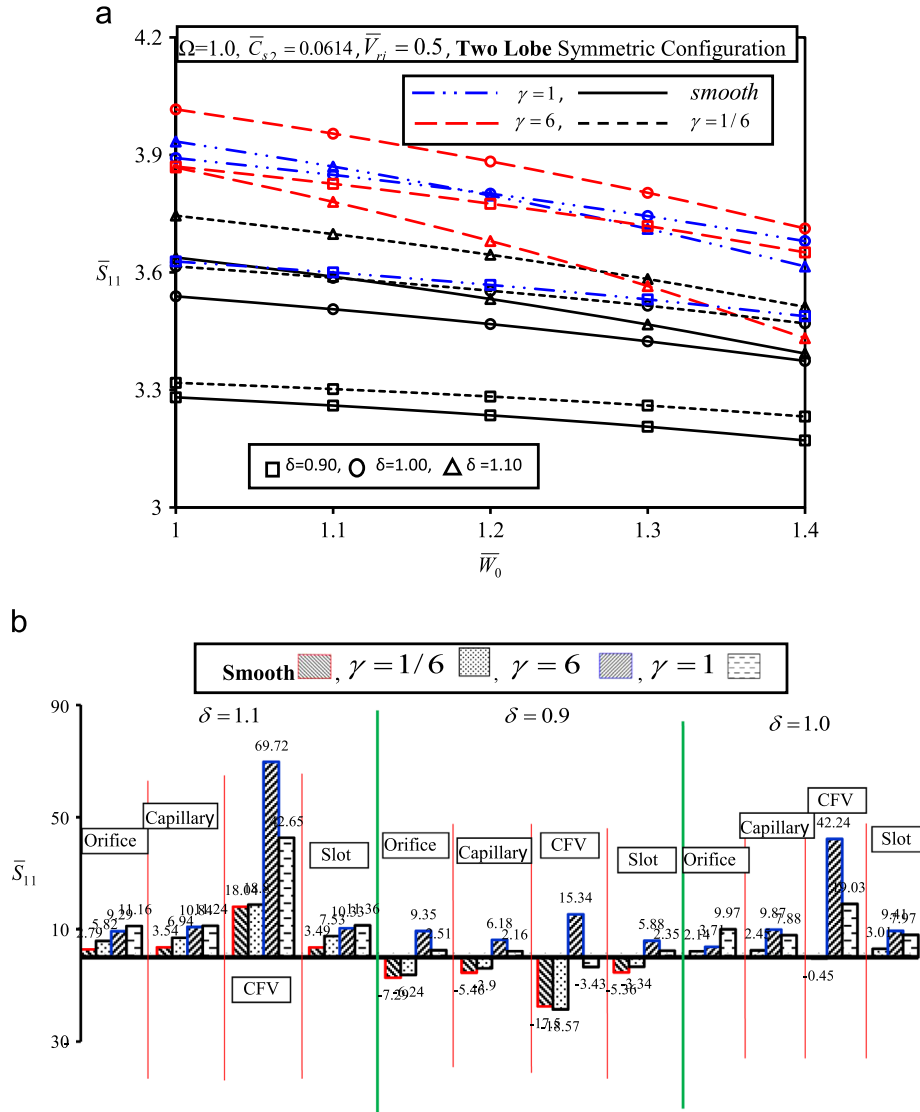


Fig. 8. (a) Variation of \bar{S}_{11} for symmetric two lobe journal bearing and (b) Percentage change in \bar{S}_{11} w.r.t base bearing for symmetric two lobe journal bearing ($\bar{W}_0 = 1.0$).

factor ($\delta \geq 1.1$). This is due to the change in the bearing geometry. Fig. 7(b) depicts the percentage change in bearing flow (\bar{Q}) for two lobe symmetric hybrid journal bearing for different surface patterns, offset factor and flow compensating elements such as an orifice, capillary and slot restrictor. The percentage change results are not presented here for the case of bearing compensated with CFV restrictor, as it is a fixed type of restrictor where the lubricant flow remains constant during the operation. From Fig. 7(b) it may be noticed that the capillary restrictor with longitudinal roughness ($\gamma=6$) and offset factor $\delta=1.1$ has the highest reduction in bearing lubricant flow of 20.27% in comparison to smooth and other roughness patterns. Further, from the restrictor selection point of view for $\gamma=6, 1$ & $1/6$, designer can use the following criteria to have an enhanced bearing performance at lower values of bearing flow (\bar{Q}). At the value of $\delta=1.1$, $\bar{Q}_{\text{Capillary}} < \bar{Q}_{\text{Slot}} < \bar{Q}_{\text{Orifice}}$ and for $\delta=1.0$, $\bar{Q}_{\text{Slot}} < \bar{Q}_{\text{Capillary}} < \bar{Q}_{\text{Orifice}}$.

In general, it may be stated that the two lobe symmetric non-recessed hybrid journal bearing in combination of longitudinal roughness pattern with offset factor $\delta > 1.0$ requires lesser lubricant supply as compared to the smooth as well as rough bearing configurations with isotropic surface orientation at a specified external load ($\bar{W}_0 = 1.0$). The bearing configurations with transverse roughness patterns, in general, show opposite behavior.

4.4. Influence on stiffness coefficients (\bar{S}_{11} , \bar{S}_{22})

Fig. 8(a) depicts the variation of direct fluid film stiffness coefficient (\bar{S}_{11}). From Fig. 8(a) it may be observed that the value of \bar{S}_{11} decreases for all the types of roughness patterns (γ) with increase in load. For a longitudinal roughness pattern ($\gamma=6$) and an isotropic roughness pattern ($\gamma=1$), the value of \bar{S}_{11} is observed to increase for offset factor $\delta \geq 1$. The notable observation from Fig. 8 (a) is that the value of the fluid film stiffness coefficient (\bar{S}_{11}) is largest for $\gamma=6$ for circular bearing than the bearing with the value of offset factor $\delta > 1$. Fig. 8(b) shows the % change in \bar{S}_{11} with respect to the base bearing for two lobe symmetric hybrid journal bearing. For a concentric design pressure ratio $\beta^* = 0.5$ and offset factor $\delta > 1$, it may be observed that the bearing compensated with CFV restrictor provides a larger value of fluid film stiffness coefficient (\bar{S}_{11}) than the bearing compensated with orifice, capillary and slot restrictors. The constant flow valve restrictor provides constant flow of lubricant at a specified value external load ($\bar{W}_0 = 1.0$) which results in not as much of displacement of journal. As a consequence of this, CFV provides a stiffer bearing system. Thus, bearing operates at higher value of \bar{S}_{11} and same trend is also observed in the value of direct fluid film stiffness coefficient (\bar{S}_{22}).

Further, it may be noticed that there is a sudden reduction in the value of \bar{S}_{11} for orifice compensated bearing than slot restrictor at

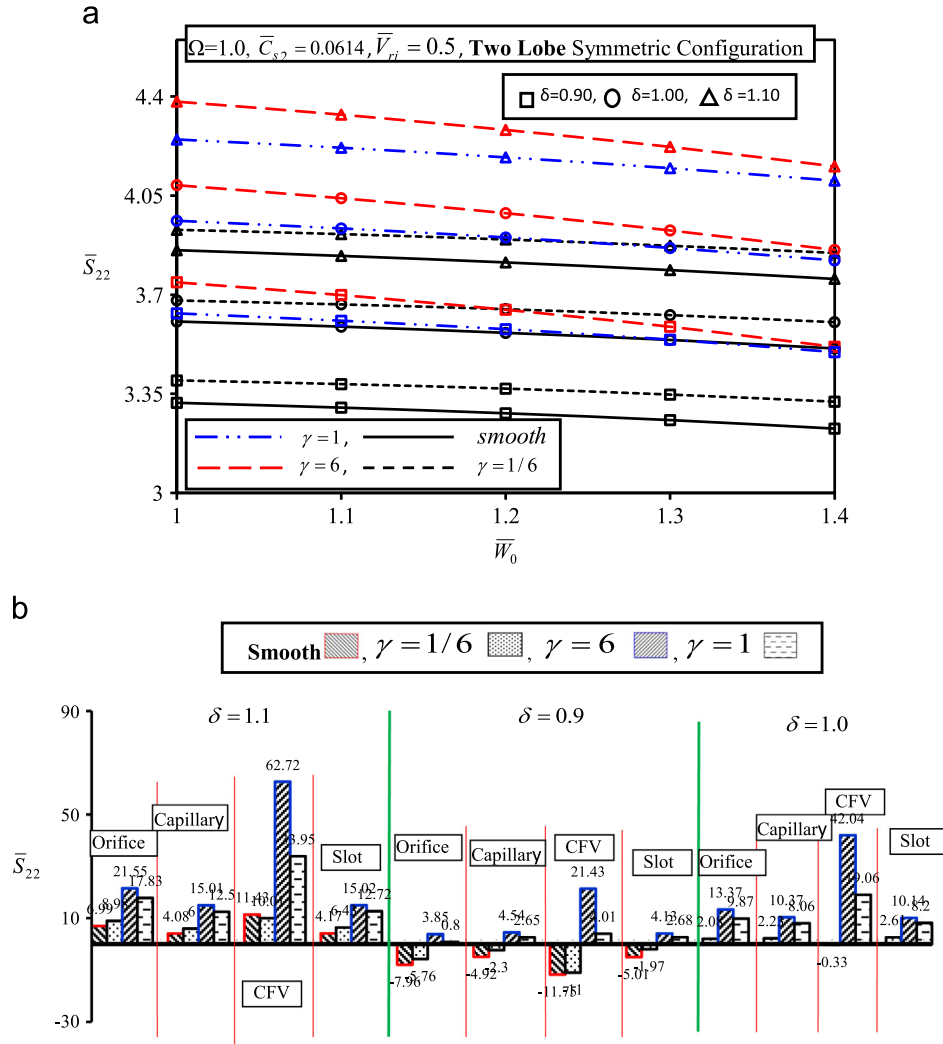


Fig. 9. (a) Variation of \bar{S}_{22} for symmetric two lobe journal bearing. (b) Percentage change in \bar{S}_{22} w.r.t base bearing for symmetric two lobe journal bearing ($\bar{W}_0 = 1.0$).

the value of offset factor $\delta = 1.1$. This is due to dispersion losses in discrete orifices and feeding holes. For $\gamma = 6$, the percentage increase in the value of \bar{S}_{11} for $\delta = 1.1$ is found to be of the order of 69.7% for CFV restrictor and 9–10% for orifice, capillary and slot restrictors. Further, it is observed that the orifice, capillary and slot restrictor compensated bearings provide larger values of \bar{S}_{11} for the isotropic roughness pattern of ($\gamma = 1$) than the longitudinal roughness pattern ($\gamma = 6$) for $\delta = 1.1$. The CFV compensated bearings for the value of $\delta = 0.9$, shows significant reduction in the value of \bar{S}_{11} (17–18%) for transverse roughness and smooth bearing. From Fig. 8 (a,b), it is observed that the roughness pattern have a significant effect on the value of fluid film stiffness coefficient (\bar{S}_{11}). For longitudinal and isotropic oriented roughness pattern, the fluid film of lubricant becomes stiffer at lower values of h/σ . However, the transverse roughness shows a reverse trend. Further, the value of direct stiffness coefficient depends upon the load capacity. The pressure generation is totally dependent on the roughness orientation pattern. The restriction on the side leakage flow is greater for longitudinal roughness pattern than transverse pattern. Because of this, the load capacity of transverse roughness pattern is lower than the longitudinal roughness pattern. As a result of this, longitudinal roughness pattern ($\gamma > 1$) provides the largest value of direct stiffness coefficients and transverse roughness pattern provides the lowest value of direct stiffness coefficients.

Further, it may be noticed that proper selection of offset factor and compensating device may compensate the reduction occurred

in the values of \bar{S}_{11} . Therefore, to improve the values of fluid film stiffness coefficient (\bar{S}_{11}), the bearing designers should opt following criteria on the basis of offset factor and compensating device. At $\delta = 1.1$, $\bar{S}_{11}|_{CFV} > \bar{S}_{11}|_{Slot} > \bar{S}_{11}|_{Capillary} > \bar{S}_{11}|_{Orifice}$ for $\gamma = 6, 1, 1/6$. The variation in the values of direct fluid film stiffness coefficient (\bar{S}_{22}) is shown in Fig. 9(a). The value of direct fluid film stiffness coefficient (\bar{S}_{22}) reduces with decrease in the value of γ . As the surface roughness changes from longitudinal ($\gamma = 6$) to more isotropic or transverse pattern ($\gamma \leq 1$), the side flow of the lubricant increases thereby decreasing the main flow. Thus resulting in reduction of direct fluid film stiffness coefficient (\bar{S}_{22}) values. Further, it may be noticed that the bearing with offset factor $\delta = 1.1$ provides highest values of direct fluid film stiffness coefficient (\bar{S}_{22}) for all surface roughness patterns. The stiffness coefficient \bar{S}_{11} too offers similar trend. The combined influence of offset factor $\delta \geq 1.0$ and roughness pattern $\gamma \geq 1$ is to increase the value of \bar{S}_{22} . The maximum increment of the order of around 16–18% and 8–9% in the values of \bar{S}_{22} is observed at $\delta = 1.1$ and $\delta = 1.0$ respectively for orifice compensated bearing. The percentage change in the value of direct fluid film stiffness coefficient (\bar{S}_{22}), is shown in Fig. 9(b). The percentage increase in the value of \bar{S}_{22} for longitudinal pattern is found to be of the order of 21.55%, 15.01%, 62.72% and 15.02% for the orifice, capillary, CFV and slot restrictions respectively.

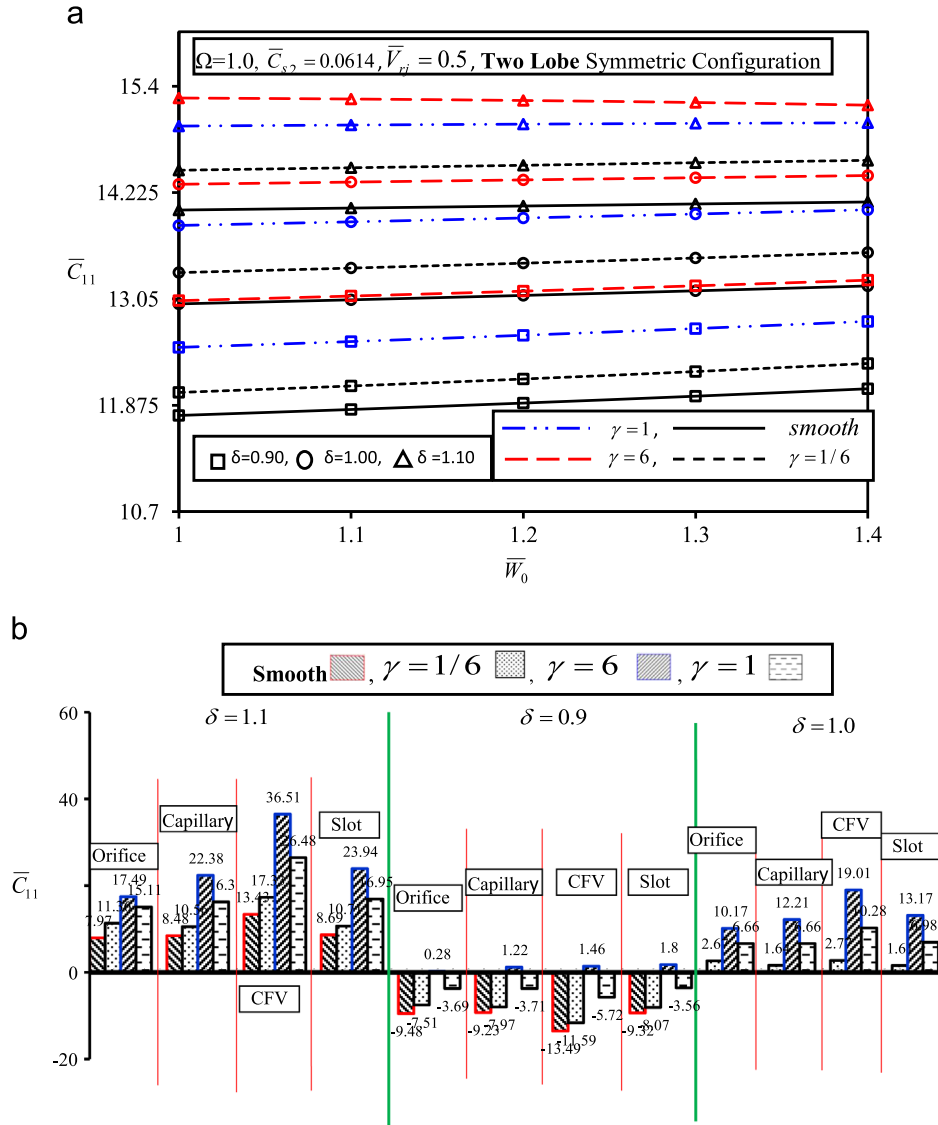


Fig. 10. (a) Variation of \bar{C}_{11} for symmetric two lobe journal bearing and (b) Percentage change in \bar{C}_{11} w.r.t base bearing for symmetric two lobe journal bearing ($\bar{W}_0 = 1.0$).

Further, the pattern of fluid film direct stiffness coefficients have been observed for all the values of offset factor (δ) and roughness pattern (γ): $\bar{S}_{22}|_{\gamma=6} > \bar{S}_{22}|_{\gamma=1} > \bar{S}_{22}|_{\gamma=1/6} > \bar{S}_{22}|_{smooth}$ and $\bar{S}_{22}|_{CFV} > \bar{S}_{22}|_{orifice} > \bar{S}_{22}|_{capillary} > \bar{S}_{22}|_{slot}$. Therefore, it is suggested that, to get desirable values of fluid film stiffness coefficients, the bearing designer is required to make a judicious selection of offset factor, roughness pattern and flow control device.

4.5. Influence of damping coefficients (\bar{C}_{11} , \bar{C}_{22})

Fig. 10(a) depicts the effects of surface pattern parameter (γ) for two sided roughness (variance ratio; $\bar{V}_{rj}=0.5$) on fluid-film damping coefficient (\bar{C}_{11}). Fig. 10(a) indicates that the value of direct fluid-film damping coefficient (\bar{C}_{11}), in general, increases with an increase in the value of the surface pattern parameter (γ). The longitudinal roughness pattern ($\gamma=6$) is observed to provide larger values of \bar{C}_{11} for all the values of offset factor. From Fig. 10(a) it is noticed that, as the value of offset factor increases, the value of direct damping coefficient (\bar{C}_{11}) also increases for all the values of roughness pattern. Fig. 10(b) indicates the percentage change in the values of direct damping coefficient (\bar{C}_{11}) for different roughness orientation patterns, offset factor and different

flow controlling devices. The longitudinal roughness pattern ($\gamma=6$) for the value of offset factor $\delta=1.1$ has highest increase in the values of direct damping coefficient \bar{C}_{11} by 36.51% when compared to the base bearing. Further, at the values of $\delta=1.0$ and 1.1 , it is observed that an increase in the value of direct damping coefficient (\bar{C}_{11}) for the longitudinal roughness pattern ($\gamma=6$) is found to be of the order of 10–17%, 12–22% 19–36% and 13–23% for the orifice, capillary, CFV and slot restrictor respectively for two lobe symmetric bearings. The bearings with transverse roughness pattern and the smooth surfaces have reported the maximum reduction in the value of the direct damping coefficient (\bar{C}_{11}) at $\delta=0.9$. It is in the order of 7–10% for orifice, capillary and slot whereas; 11–13% for CFV restrictor respectively. The variation of the direct fluid film damping coefficient (\bar{C}_{22}) is depicted in Fig. 11(a). As the value of offset factor increases from 0.9 to 1.1, enhancement in the value of direct damping coefficient (\bar{C}_{22}) is observed. This is due to the change in non-circularity of bearing. Further, the longitudinal roughness pattern shows the largest value of \bar{C}_{22} and similar trend is observed for all the values of offset factor. For orifice restrictor compensated bearing, the value of \bar{C}_{22} is increased by an order of 14.86%, 11.86%, 7.69% and 4.99% for longitudinal, isotropic, transverse and smooth roughness pattern respectively when compared

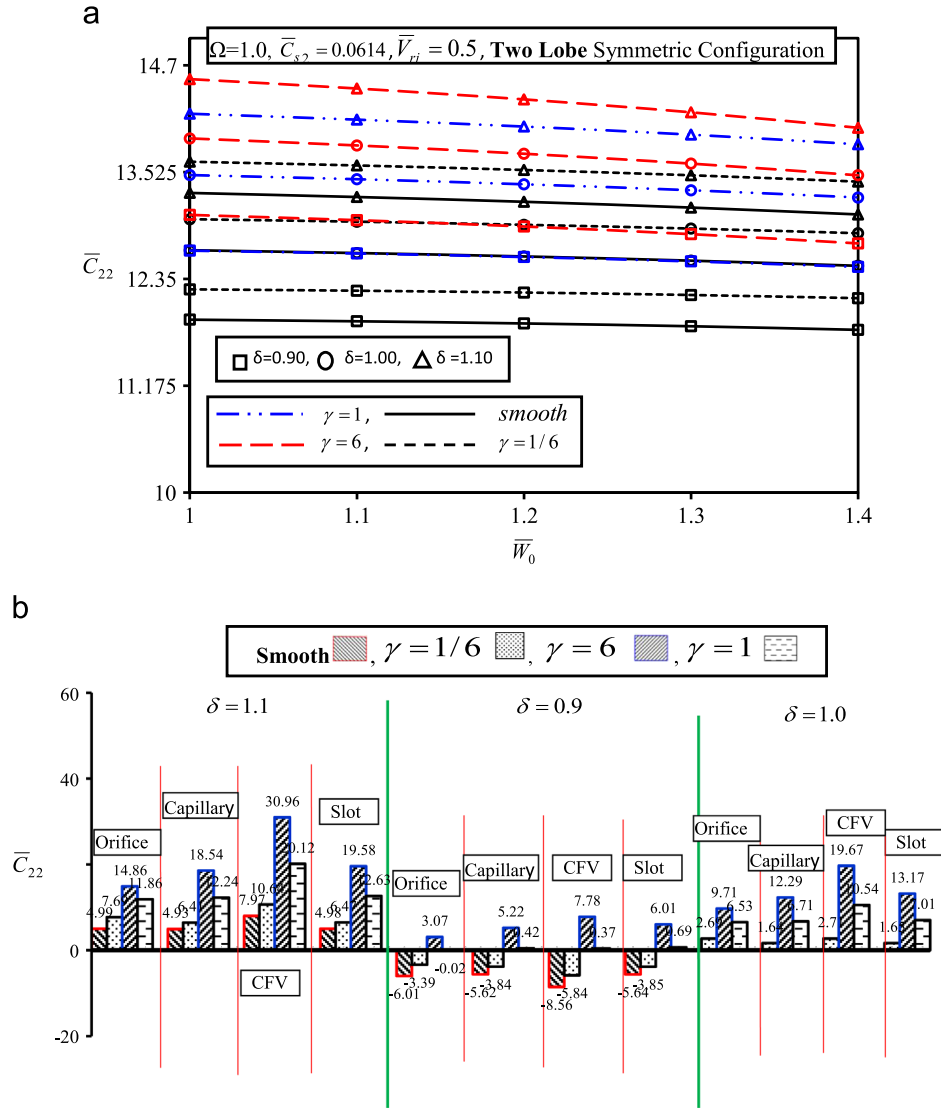


Fig. 11. (a) Variation of \bar{C}_{22} for symmetric two lobe journal bearing. (b) Percentage change in \bar{C}_{22} w.r.t base bearing for symmetric two lobe journal bearing ($\bar{W}_0 = 1.0$).

with the base bearing at $\delta=1.1$. From Fig. 11(a), it is clearly noticeable that the influence of roughness pattern ($\gamma \geq 1$) is to increase the value of \bar{C}_{22} . The value of \bar{C}_{22} is being minimum for the smooth bearing surface at $\delta=0.9$. Fig. 11(b) depicts the percentage change in the values of \bar{C}_{22} for symmetric bearing compensated with different restrictors. From Fig. 11(b), it may be observed that the CFV compensated bearing provides the largest value of \bar{C}_{22} than the bearing compensated with orifice, capillary and slot restrictors. The maximum percentage increase in the values of \bar{C}_{22} is observed in the order of 30.96%, 18.54%, 19.58% and 14.86% at $\delta=1.1$ and $\gamma=6$ for CFV, slot, capillary and orifice compensated bearings respectively. The influence of surface roughness in general, is to increase the value of direct damping coefficient (\bar{C}_{22}) compared to smooth journal bearing. It is observed that, the longitudinal ($\gamma=6$) roughness pattern has a highest percentage increase i.e. 17% in the values of \bar{C}_{22} for the value of an external load $\bar{W}_0=1.1$. The following trend has been observed in the value of \bar{C}_{22} for all the values of offset factor for the case of symmetric two lobe bearing $\bar{C}_{22}|_{\gamma=6} > \bar{C}_{22}|_{\gamma=1} > \bar{C}_{22}|_{smooth} > \bar{C}_{22}|_{\gamma=1/6}$. From the point of view of damping out the oscillations, CFV compensated bearing with longitudinal roughness pattern at the value of offset factor $\delta=1.1$ is observed to be better as it provides higher values of \bar{C}_{11} and \bar{C}_{22} for two lobe symmetric bearing.

4.6. Influence on threshold speed ($\bar{\omega}_{th}$)

Fig. 12(a) shows the variation in stability threshold speed margin ($\bar{\omega}_{th}$) with respect to external load (\bar{W}_0) for an orifice compensated symmetric bearing configuration for different surface roughness patterns. The value of $\bar{\omega}_{th}$ is observed to decrease with increase in external load for all roughness patterns. From Fig. 12(a), it may be observed that an increase in the value of roughness pattern (γ) from $1/6$ to 6 , results in an increase in the value of stability threshold speed margin ($\bar{\omega}_{th}$) for all the values of offset factor. This is due to the change in rotor dynamic coefficients owing to the roughness patterns. Further, it may be noticed that, for a given value of an external load (\bar{W}_0), the longitudinal roughness pattern provides the largest value of stability threshold speed margin ($\bar{\omega}_{th}$) and smooth and transverse roughness provides the minimum value of $\bar{\omega}_{th}$ at all offset factors ($\delta=1.1, 1.0, 0.9$). The percentage change in the value of $\bar{\omega}_{th}$ at $\delta=1.1, \gamma=6$ for orifice restrictor is found to be of the order of 7.46% for two lobe bearing with respect to smooth surface circular non-recessed hybrid bearing.

Fig. 12(b) indicates percentage change in the value of stability threshold speed margin ($\bar{\omega}_{th}$) for different roughness patterns, offset factor and different flow controlling devices for symmetric bearing configuration. From Fig. 12(b), it may be observed that the value of $\bar{\omega}_{th}$ is found to be largest for the case CFV compensated

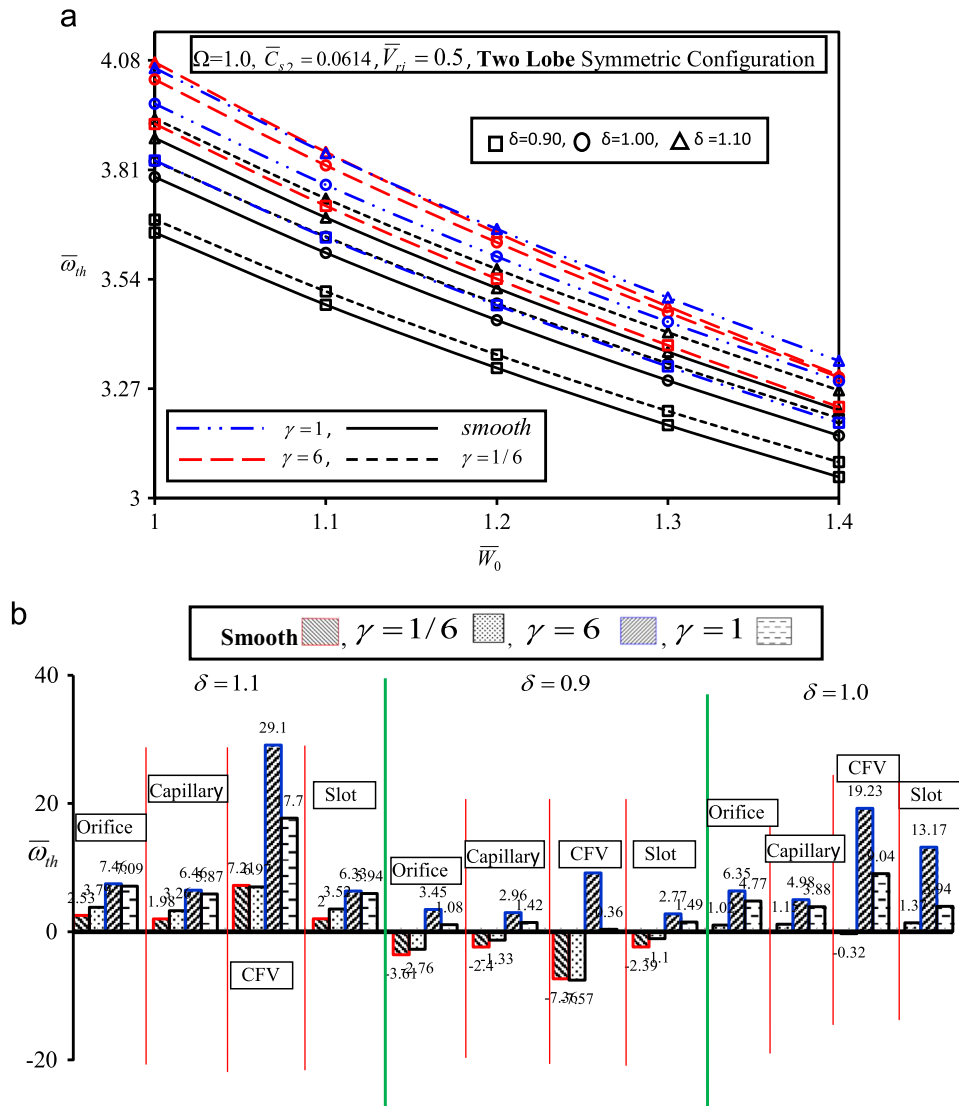


Fig. 12. (a) Variation of $\bar{\omega}_{th}$ for symmetric two lobe journal bearing and (b) Percentage change in $\bar{\omega}_{th}$ w.r.t base bearing for symmetric two lobe journal bearing ($\bar{W}_0 = 1.0$).

bearing than that of other compensated bearings and is found to be the order of around 29.10% for bearings with longitudinal roughness pattern ($\gamma=6$). This is due to higher value of rotor dynamic coefficients for CFV at longitudinal roughness patterns. As a result of this, the largest value of $\bar{\omega}_{th}$ is anticipated for CFV than that of other restrictors. For the value of roughness pattern $\gamma=6$ and $\gamma=1$; the change in the value of stability threshold speed margin ($\bar{\omega}_{th}$) is observed to be marginal. Thus, for longitudinal and isotropic roughness pattern, the selection of appropriate bearing geometry and type of restrictor have a significant effect on the value of stability threshold speed margin ($\bar{\omega}_{th}$). Therefore, in order to have an enhanced value of stability threshold speed margin ($\bar{\omega}_{th}$), the bearing designer may choose a proper bearing configuration.

From the stability point of view, to have an enhanced value of $\bar{\omega}_{th}$, the bearing designer should make a judicious selection of these factors from the following criterion:

$$\bar{\omega}_{th} \begin{matrix} \delta = 1.1, 1.0, 0.9 \\ \bar{W}_0 = 1.0 \\ \gamma = 6.0 \\ \text{Orifice, Capillary, Slot} \\ \text{Symmetric} \end{matrix} > \bar{\omega}_{th} \begin{matrix} \delta = 1.1, 1.0, 0.9 \\ \bar{W}_0 = 1.0 \\ \gamma = 1.0 \\ \text{Orifice, Capillary, Slot} \\ \text{Symmetric} \end{matrix}$$

$$> \bar{\omega}_{th} \begin{matrix} \delta = 1.1, 1.0, 0.9 \\ \bar{W}_0 = 1.0 \\ \text{smooth} \\ \text{Orifice, Capillary, Slot} \\ \text{Symmetric} \end{matrix} > \bar{\omega}_{th} \begin{matrix} \delta = 1.1, 1.0, 0.9 \\ \bar{W}_0 = 1.0 \\ \gamma = 1/6 \\ \text{Orifice, Capillary, Slot} \\ \text{Symmetric} \end{matrix}$$

$$\bar{\omega}_{th} \begin{matrix} \delta = 1.1, 1.0, 0.9 \\ \bar{W}_0 = 1.0 \\ \gamma = 6.0 \\ \text{CFV} \\ \text{Symmetric} \end{matrix} > \bar{\omega}_{th} \begin{matrix} \delta = 1.1, 1.0, 0.9 \\ \bar{W}_0 = 1.0 \\ \gamma = 1.0 \\ \text{CFV} \\ \text{Symmetric} \end{matrix}$$

$$> \bar{\omega}_{th} \begin{matrix} \delta = 1.1, 1.0, 0.9 \\ \bar{W}_0 = 1.0 \\ \gamma = 1/6 \\ \text{CFV} \\ \text{Symmetric} \end{matrix} > \bar{\omega}_{th} \begin{matrix} \delta = 1.1, 1.0, 0.9 \\ \bar{W}_0 = 1.0 \\ \text{smooth} \\ \text{CFV} \\ \text{Symmetric} \end{matrix}$$

Table 2

Bearing performance characteristic parameters for different surface orientation parameter and offset factor (symmetric bearing configuration).

External load	Offset factor (δ)	Surface orientation parameter (γ)	\bar{h}_{\min}				\bar{S}_{22}				\bar{C}_{11}				$\bar{\omega}_{th}$			
			Orifice	Capillary	CFV	Slot	Orifice	Capillary	CFV	Slot	Orifice	Capillary	CFV	Slot	Orifice	Capillary	CFV	Slot
1.4	1.1	Smooth	0.7565	0.7173	0.8079	0.7243	3.756	2.981	6.127	2.958	14.122	11.923	20.111	12.498	3.217	2.895	4.271	2.876
		$\gamma = 1/6$	0.7607	0.7320	0.8096	0.7249	3.848	2.900	6.069	3.027	14.580	12.921	20.830	12.67	3.266	2.926	4.263	2.8
		$\gamma = 6$	0.7718	0.7366	0.835	0.7494	4.153	3.271	8.856	3.245	15.191	13.411	24.041	14.202	3.303	2.965	5.118	2.918
		$\gamma = 1$	0.7685	0.7419	0.823	0.6981	4.103	3.311	7.349	3.196	14.996	12.517	22.371	13.48	3.339	3.030	4.681	2.901
	0.9	Smooth	0.8278	0.7894	0.872	0.7947	3.227	2.725	4.896	2.702	12.058	10.052	15.525	10.507	3.052	2.773	3.708	2.753
		$\gamma = 1/6$	0.8325	0.7938	0.8759	0.7992	3.322	2.813	4.961	2.801	12.337	10.193	15.887	10.646	3.089	2.810	3.702	2.797
		$\gamma = 6$	0.8447	0.8117	0.8946	0.8191	3.516	2.96	6.655	2.932	13.258	11.186	18.063	11.786	3.225	2.905	4.346	2.879
		$\gamma = 1$	0.839	0.8027	0.8848	0.8094	3.497	2.937	5.76	2.917	12.801	10.662	16.875	11.173	3.186	2.877	4.011	2.858
	1.0	Smooth	0.8058	0.7613	0.8583	0.771	3.51	2.864	5.518	2.841	13.194	11.021	17.818	11.531	3.154	2.840	3.991	2.82
		$\gamma = 1/6$	0.8105	0.7656	0.861	0.7753	3.603	2.939	5.521	2.925	13.563	11.203	18.335	11.71	3.197	2.878	3.980	2.865
		$\gamma = 6$	0.8263	0.7865	0.8883	0.7965	3.858	3.131	7.752	3.104	14.413	12.351	21.049	13.05	3.298	2.965	4.736	2.939
		$\gamma = 1$	0.8197	0.7769	0.8747	0.7865	3.821	3.090	6.557	3.07	14.035	11.756	19.600	12.338	3.289	2.945	4.346	2.926
1.0	1.1	Smooth	0.801	0.772	0.8361	0.7784	3.857	2.98	5.943	2.947	14.032	11.635	19.724	12.157	3.888	3.439	4.966	3.414
		$\gamma = 1/6$	0.8039	0.775	0.8372	0.7814	3.929	3.035	5.867	3.011	14.472	11.858	20.403	12.382	3.936	3.482	4.955	3.465
		$\gamma = 6$	0.8128	0.7863	0.8558	0.7936	4.382	3.293	8.678	3.254	15.269	13.126	23.738	13.862	4.075	3.59	5.98	3.559
		$\gamma = 1$	0.8099	0.7819	0.847	0.7885	4.248	3.221	7.144	3.189	14.959	12.474	21.993	13.08	4.061	3.57	5.452	3.546
	0.9	Smooth	0.881	0.8527	0.9118	0.8581	3.318	2.722	4.706	2.687	11.763	9.735	15.041	10.141	3.655	3.291	4.291	3.267
		$\gamma = 1/6$	0.8842	0.8555	0.9145	0.8609	3.397	2.797	4.746	2.773	12.018	9.87	15.372	10.281	3.687	3.327	4.281	3.31
		$\gamma = 6$	0.8936	0.8686	0.9283	0.8748	3.744	2.993	6.476	2.946	13.032	10.856	17.643	11.386	3.923	3.472	5.056	3.44
		$\gamma = 1$	0.8891	0.8619	0.9211	0.8676	3.634	2.939	5.547	2.905	12.515	10.327	16.393	10.785	3.833	3.42	4.649	3.397
	1.0	Smooth	0.8616	0.8288	0.8978	0.8355	3.605	2.863	5.333	2.829	12.995	10.725	17.388	11.184	3.792	3.372	4.632	3.347
		$\gamma = 1/6$	0.8648	0.8317	0.8996	0.8385	3.68	2.927	5.315	2.903	13.342	10.901	17.87	11.365	3.831	3.411	4.617	3.393
		$\gamma = 6$	0.877	0.8472	0.9197	0.854	4.087	3.16	7.575	3.116	14.317	12.035	20.695	12.658	4.033	3.54	5.523	3.508
		$\gamma = 1$	0.8718	0.84	0.9097	0.8467	3.961	3.094	6.35	3.061	13.861	11.44	19.176	11.965	3.973	3.503	5.051	3.479

Table 3Performance percentage change for two lobe symmetric non-recessed hybrid journal bearing ($\bar{W}_0 = 1.4$).

δ	Surface orientation parameter (γ)	\bar{P}_{\max}				\bar{h}_{\min}				\bar{S}_{11}				\bar{S}_{22}			
		Orifice	Capillary	CFV	Slot	Orifice	Capillary	CFV	Slot	Orifice	Capillary	CFV	Slot	Orifice	Capillary	CFV	Slot
1.1	Smooth	5.25	4.56	7.95	4.09	−6.11	−5.77	−5.87	−6.05	0.56	3.63	17.72	4.07	7.00	4.08	11.03	4.11
	$\gamma = 1/6$	4.25	−1.77	6.24	−2.29	−5.59	−3.84	−5.67	−5.97	4.09	5.62	18.79	8.27	9.62	1.25	9.98	6.54
	$\gamma = 6$	16.66	22.47	28.68	12.09	−4.21	−3.24	−2.71	−2.80	1.71	8.69	67.6	9.41	18.31	14.21	60.49	14.22
	$\gamma = 1$	9.87	13.56	15.29	7.04	−4.62	−2.54	−4.11	−9.45	7.14	9.40	41.91	10.97	16.89	15.60	33.18	12.49
0.9	Smooth	0.96	2.007	−0.92	0.94	2.73	3.69	1.59	3.07	−6.01	−5.58	−17.24	−5.60	−8.06	−4.85	−11.2	−4.89
	$\gamma = 1/6$	0.75	2.19	−1.51	0.97	3.31	4.26	2.05	3.65	−4.20	−3.37	−18.09	−2.82	−5.35	−1.78	−10.0	−1.40
	$\gamma = 6$	9.98	9.15	12.45	0.99	4.82	6.62	4.22	6.23	8.20	4.19	14.55	3.65	0.17	3.35	20.60	3.20
	$\gamma = 1$	4.88	5.39	4.20	4.36	4.12	5.43	3.08	4.98	3.37	1.61	−3.34	1.67	−0.37	2.54	4.38	2.67
1.0	Smooth	−	−	−	−	−	−	−	−	−	−	−	−	−	−	−	−
	$\gamma = 1/6$	−1.73	−1.11	−2.69	−1.11	0.58	0.56	0.31	0.55	2.84	3.11	−0.18	3.73	2.64	2.61	0.054	2.95
	$\gamma = 6$	10.79	8.24	17.70	7.95	2.54	3.31	3.49	3.30	3.71	8.20	40.86	7.62	9.91	9.32	40.48	9.25
	$\gamma = 1$	3.90	3.18	5.75	3.10	1.72	2.04	1.91	2.01	9.06	7.49	18.73	7.58	8.86	7.89	18.82	8.06

δ	Surface orientation parameter (γ)	\bar{C}_{11}				\bar{C}_{22}				\bar{w}_{th}			
		Orifice	Capillary	CFV	Slot	Orifice	Capillary	CFV	Slot	Orifice	Capillary	CFV	Slot
1.1	Smooth	7.03	8.18	12.86	8.38	4.51	4.72	7.77	4.75	1.99	1.93	7.01	1.94
	$\gamma = 1/6$	10.50	17.23	16.90	9.87	7.41	14.90	10.49	6.11	3.55	3.02	6.81	−0.70
	$\gamma = 6$	15.13	21.68	34.92	23.16	12.14	18.42	30.40	19.190	4.72	4.40	28.23	3.47
	$\gamma = 1$	13.65	13.57	25.55	16.90	10.70	11.57	19.85	12.12	5.86	6.69	17.28	2.87
0.9	Smooth	−8.60	−8.79	−12.86	−8.88	−5.64	−5.36	−8.31	−5.34	−3.23	−2.35	−7.09	−2.37
	$\gamma = 1/6$	−6.49	−7.51	−10.83	−7.67	−2.85	−3.52	−5.48	−3.52	−2.06	−1.05	−7.24	−0.81
	$\gamma = 6$	0.48	1.49	1.37	2.21	1.96	5.36	7.76	6.28	2.25	2.28	8.89	2.09
	$\gamma = 1$	−2.97	−3.25	−5.29	−3.10	−0.09	0.74	0.61	1.06	1.01	1.30	0.50	1.34
1.0	Smooth	−	−	−	−	−	−	−	−	−	−	−	−
	$\gamma = 1/6$	2.79	1.65	2.90	1.55	2.86	1.67	2.78	1.65	1.36	1.33	−0.27	1.59
	$\gamma = 6$	9.23	12.06	18.13	13.17	7.97	12.13	19.35	13.09	4.56	4.40	18.66	4.21
	$\gamma = 1$	6.37	6.669	10.0	6.99	6.00	6.73	10.50	7.04	4.28	3.69	8.89	3.75

$$\bar{\omega}_{th} \left| \begin{array}{c} \delta = 1.1 \\ \bar{W}_0 = 1.0 \\ \gamma = 6.0 \\ CFV \end{array} \right. > \bar{\omega}_{th} \left| \begin{array}{c} \delta = 1.1 \\ \bar{W}_0 = 1.0 \\ \gamma = 6.0 \\ Orifice \end{array} \right. > \bar{\omega}_{th} \left| \begin{array}{c} \delta = 1.1 \\ \bar{W}_0 = 1.0 \\ \gamma = 6.0 \\ Capillary \end{array} \right. > \bar{\omega}_{th} \left| \begin{array}{c} \delta = 1.1 \\ \bar{W}_0 = 1.0 \\ \gamma = 6.0 \\ Slot \end{array} \right.$$

For the sake of brevity and to have a better physical insight; the computed results for external load $\bar{W}_0 = 1.4$ and the percentage change due to the influence of surface roughness on the bearing performance characteristics viz. \bar{P}_{max} , \bar{h}_{min} , \bar{S}_{11} , \bar{S}_{22} , \bar{C}_{11} , \bar{C}_{22} and $\bar{\omega}_{th}$ have been presented in Table 2 and Table 3 respectively for two lobe symmetric bearing. The computed results of the study presented in Table 2 and Table 3 reveals that surface pattern parameter, offset factor and flow controlling elements have a noteworthy influence in the improvement of the bearing performance and must be included in the analysis for realistic generation of bearing characteristics data.

5. Conclusion

A theoretical study to investigate the effect of surface roughness on the performance of two lobe non-recessed hybrid journal bearings compensated with different types of flow control devices such as orifice, capillary, constant flow valve and slot entry restrictors, has been performed. Based on the numerically simulated results presented for different forms of surface roughness patterns, following conclusions have been drawn:

1. The value of minimum fluid film thickness (\bar{h}_{min}) reduces as the value of the surface roughness pattern parameter (γ) decreases. An increase in offset factor (δ) is seen to increase the value of \bar{h}_{min} . The longitudinal roughness ($\gamma = 6$) pattern provides an improved value of \bar{h}_{min} whereas, a transverse roughness pattern provides a smaller value. However, use of orifice restrictor may compensate the reduction in the value of \bar{h}_{min} partially than the CFV, capillary and slot entry compensating devices for the same operating condition.
2. The values of direct fluid film stiffness coefficients (\bar{S}_{11} , \bar{S}_{22}) get enhanced for longitudinal roughness pattern ($\gamma = 6$) for the chosen values of offset factor (δ). A bearing compensated with CFV restrictor provides the largest value of stiffness coefficients (\bar{S}_{11} , \bar{S}_{22}) for $\gamma = 6$, 1 and $\gamma = 1$. However, a reduction in the values of direct fluid film stiffness coefficient is observed for transverse roughness pattern and smooth surface. Following pattern has been obtained for the value of direct fluid film stiffness coefficients (\bar{S}_{11} , \bar{S}_{22}):

$$\bar{S}_{11}|_{CFV} > \bar{S}_{11}|_{Slot} > \bar{S}_{11}|_{Capillary} > \bar{S}_{11}|_{Orifice} \text{ and } \bar{S}_{22}|_{CFV} > \bar{S}_{22}|_{Orifice} > \bar{S}_{22}|_{Capillary} > \bar{S}_{22}|_{Slot}$$

$$\bar{S}_{11}/\bar{S}_{22}|_{\gamma=6} > \bar{S}_{11}/\bar{S}_{22}|_{\gamma=1} > \bar{S}_{11}/\bar{S}_{22}|_{\gamma=1/6} > \bar{S}_{11}/\bar{S}_{22}|_{smooth} \text{ at } \delta = 1.1$$
3. For a two lobe non-recessed symmetric constant flow valve compensated bearing, largest value of direct fluid-film damping coefficient (\bar{C}_{11} , \bar{C}_{22}) is observed for longitudinal roughness pattern ($\gamma = 6$) when the value of offset factor is greater than one ($\delta \geq 1$). This is followed by slot, capillary and orifice restrictor bearings. For different roughness pattern, the following trend has been observed for the value of \bar{C}_{11} and \bar{C}_{22} :

$$\bar{C}_{11}|_{\gamma=6} > \bar{C}_{11}|_{\gamma=1} > \bar{C}_{11}|_{\gamma=1/6} > \bar{C}_{11}|_{smooth} \text{ and } \bar{C}_{22}|_{\gamma=6}$$

$$> \bar{C}_{22}|_{\gamma=1} > \bar{C}_{22}|_{smooth} > \bar{C}_{22}|_{\gamma=1/6}$$

4. For a two lobe journal bearing system, the longitudinal and isotropic roughness pattern ($\gamma \geq 1$) along with the offset factor $\delta \geq 1$ seems to be better from the stability threshold speed margin ($\bar{\omega}_{th}$) point of view. An appropriate selection of compensating device may provide enhanced values of stability threshold speed margin ($\bar{\omega}_{th}$).
5. From the study of two lobe non-recessed hybrid bearing, it is revealed that a judicious selection of parameters such as surface pattern parameter (γ), offset factor (δ) in conjunction with type of flow control device is desirable to get an improved bearing performance.

References

- [1] Rowe WB, Xu SX, Chong FS, Weston W. Hybrid journal bearings with particular reference to hole-entry configuration. *Tribol Int* 1982;15(6):339–48.
- [2] Stout KJ, Rowe WB. Externally pressurized bearings design for manufacture Part I – journal bearing selection. *Tribol Int* 1974;7(3):98–106.
- [3] Sharma Satish C, Kumar V, Jain SC, Sinhasan R, Subramanian M. A study of slot-entry hydrostatic/hybrid journal bearing using the finite element method. *Tribol Int* 1999;32:185–96.
- [4] Nagaraju T, Sharma Satish C, Jain SC. Influence of surface roughness effects on the performance of non recessed hybrid journal bearings. *Tribol Int* 2002;35(7):467–87.
- [5] Phalle Vikas M, Sharma Satish C, Jain SC. Performance analysis of 2-lobe worn multirecess hybrid journal bearing system using different flow control devices. *Tribol Int* 2012;52:101–16.
- [6] Nagaraju T, Sharma Satish C, Jain SC. Study of orifice compensated hole-entry hybrid journal bearing considering surface roughness and flexibility effects. *Tribol Int* 2006;39(7):715–25.
- [7] Pinkus O. Analysis of elliptical bearing. *ASME Trans* 1956;78:965–73.
- [8] Dowson D. A generalized Reynolds equation for fluid film lubrication. *Int J Mech Eng Sci* 1962;4(2):159–70.
- [9] Lund JW, Thomsen KK. A calculation method and data for the dynamic coefficient of oil lubricated journal bearing. In: *ASME design engineering conference*, Chicago: ASME; 1978. 100118: p. 1–28.
- [10] Garner DR, Lee CS, Martin FA. Stability of profile bore bearing: influence of bearing type selection. *Tribol Int* 1980;13(5):204–10.
- [11] Goenka PK, Booker JF. Effect of surface ellipticity on dynamically loaded cylindrical bearing. *ASME, J Lubr Technol* 1983;1–12.
- [12] Malik M. A comparative study of some two lobed journal bearing configurations. *ASLE Trans* 1983;26(1):118–24.
- [13] Sinhasan R, Goyal KC. Transient response of a two-lobe journal bearing lubricated with non-newtonian lubricant. *Tribol Int* 1995;28(4):233–9.
- [14] Bouyer J, Fillon M, Pierre-Danos I. Influence of wear on the behavior of a two-lobe hydrodynamic journal bearing subjected to numerous start ups and stops. *ASME, J Tribol*, 129; 2007; 205–8.
- [15] Rahmatabadi AD, Nekoeimehr M, Rashidi R. Micropolar lubricant effects on the performance of noncircular lobed bearings. *Tribol Int* 2010;43(1–2):404–413.
- [16] San Andres L. A hybrid radial bearing with improved rotor dynamic stability. In: *Proceedings of the international symposium on stability control of rotating machinery*, South Lake Tahoe: California, USA; 2001.
- [17] Ghosh MK, Satish MR. Rotor dynamic characteristics of multi lobe hybrid bearings with short sills—Part I. *Tribol Int* 2003;36(8):625–32.
- [18] Ghosh MK, Satish MR. Rotor dynamic characteristics of multilobe hybrid bearings with short sills—Part II. *Tribol Int* 2003;36(8):633–6.
- [19] Phalle Vikas M, Sharma Satish C, Jain SC. Influence of wear on the performance of a 2-lobe multirecess hybrid journal bearing system compensated with membrane restrictor. *Tribol Int* 2011;44(4):380–95.
- [20] Sharma Satish C, Phalle VM, Jain SC. Performance of a noncircular 2-lobe multirecess hydrostatic journal bearing with wear. *Ind Lubr Tribol* 2012;64(3):171–81.
- [21] Sharma SC, Phalle VM, Jain SC. Combined influence of wear and misalignment of journal on the performance analysis of three-lobe three-pocket hybrid journal bearing compensated with capillary restrictor. *Trans ASME J Tribol* 2012;134(1) (011703-1–011703-11).
- [22] Basavaraja J, Sharma SC, Jain SC. A study of misaligned roughened two-lobe hole-entry hybrid journal bearing. *Ind Lubr Tribol* 2009;61(4):220–7.
- [23] Kushare Prashant B, Satish C, Sharma A. Study of two lobe non recessed worn journal bearing operating with non-Newtonian lubricant. *Proc IMechE Part J: J Eng Tribol* 2013;227(12):1418–37.
- [24] Kushare Prashant B, Sharma Satish C. Nonlinear transient stability study of two lobe symmetric hole entry worn hybrid journal bearing operating with non-Newtonian lubricant. *Tribol Int* 2014;69:84–101.
- [25] Christensen H. Stochastic models for hydrodynamic lubrication of rough surfaces. *Proc of IMechE Part 1* 1969–70;184(1):1013–26.

- [26] Christensen H, Tonder K. The hydrodynamic lubrication of rough journal bearings. *Trans ASME, J Lubr Technol* 1973;95(2):166–72.
- [27] Turaga R, Sekhar AS, Majumdar BC. Unbalance response and stability of a rotor supported on hydrodynamic journal bearings with rough surfaces. *IMechE, Part J, J Eng Tribol* 1999;213(1):31–4.
- [28] Patir N, Cheng HS. An average flow model for determining effect of three-dimensional roughness on partial hydrodynamic lubrication. *Trans ASME J Lubr Technol* 1978;100(1):12–7.
- [29] Patir N, Cheng HS. Application of average flow model to lubrication between rough sliding surfaces. *Trans ASME J Lubr Technol* 1979;101(2):220–9.
- [30] Ramesh J, Majumdar BC, Rao NS. Thermohydrodynamic analysis of submerged oil journal bearing considering surface roughness effects. *Trans ASME J Tribol* 1997;119(1):100–6.
- [31] Majumdar BC, Ghosh MK. Stability of a rigid rotor supported on rough oil journal bearings. *Trans ASME J Tribol* 1990;112(1):73–7.
- [32] Guha SK. Analysis of steady-state characteristics of misaligned hydrodynamic journal bearings with isotropic roughness effect. *Tribol Int* 2000;33(1):1–12.
- [33] Jagadeesha KM, Nagaraju T, Sharma Satish C, Jain SC. 3-D surface roughness effects on transient non-Newtonian response of dynamically loaded journal bearings. *STLE, Tribol Trans* 2012;55(1):32–42.
- [34] San Andres L. Turbulent hybrid bearings with fluid inertia effects. *Trans ASME J Tribol* 1990;112(4):699–707.
- [35] Fayolle P, Childs DW. Rotor dynamic evaluation of a roughened-land hybrid bearing. *Trans ASME J Tribol* 1999;121:133–8.
- [36] Nagaraju T, Sharma SC, Jain SC. Influence of surface roughness on non-Newtonian thermo hydrostatic performance of a hole-entry hybrid journal bearing. *ASME J Tribol* 2007;129(3):595–602.
- [37] Weyler ME, Chih Wu. A Numerical method for the calculation of lubricant pressures in bearings with mixed lubrication. *Tribol Int* 1982;15(2):89–95.
- [38] Hashimoto H. Surface roughness effects in high-speed hydrodynamic journal bearings. *Trans ASME J Tribol* 1997;119(4):776–80.